Chapter 3: Heavy metal interactions in *Deinococcus sp.*

A scientist in his laboratory is not a mere technician: he is also a child confronting natural phenomena that impress him as though they were fairy tales – Marie Curie

3.1 Introduction

The production of energy from nuclear power plants, uranium mining, nuclear weapons production and nuclear accidents are the major causes of release of radionuclides into the environment. The nuclear wastes typically contain inorganic and organic contaminants that include radionuclides, heavy metals, acids/bases and solvents. The nuclear wastes are pre-dominantly contaminated with radionuclides such as uranium, plutonium, caesium, organopollutants (e.g. toluene, benzene, ethylbenzene, xylene etc.), and heavy metals (lead, mercury, chromium, arsenic and cadmium) (NABIR primer 3; Daly, 2000). The high radiation levels, in combination with the chemical hazards, causes extreme damage to ecosystem and living organisms.

The cleanup of nuclear waste by physico-chemical methods is impractical and the cost is prohibitive. A less expensive *in situ* bioremediation technology is being investigated as a potential alternative method for treating such contaminated sites. Generally, bacteria used for bioremediation are selected to target a specific form and oxidation state of toxic pollutants, such as reduction of soluble hexavalent uranium or degradation of a specific hydrocarbon. However, since radioactive waste sites are rarely contaminated by a single chemical, it is necessary for the bioremediating strain to be multi-resistant to various toxic agents. These vast waste sites are therefore potential targets for utilizing specialized microorganisms that have the ability to survive and to catalyze the desired function(s) under radiation stress.

The development of bioremediation strategies using *Deinococcus* sp., the members which are among the most radiation resistant organisms known, are therefore vital for the clean up of radioactive waste sites. Additional advanteges of deinococci are that they are vegetative, easily cultured and nonpathogenic. Due to the common presence of toxic heavy metals in waste sites, there exists a considerable interest in studying physiology and the genes involved in metal resistance and reduction for the common metallic waste constituents.

D. radiodurans can naturally reduce Cr^{6+} to less mobile and less toxic form Cr^{3+} (Fredrickson et al., 2000). Additionally, genes from other organisms are being expressed in deinococci to see whether they can impart resistance as well as develop ability to transform those metals. Brim et al., (2000) have generated *D. radiodurans* strains expressing the cloned Hg^{2+} resistance gene (*merA*) from *Escherichia coli*

BL308. *MerA* encodes mercuric ion reductase, which reduces highly toxic, thiol-reactive mercuric ion, Hg^{2+}, to less toxic and inert elemental and volatile Hg^{0}. The strains were shown to grow in the presence of both radiation and ionic mercury at concentrations well above those found in radioactive waste sites, and to effectively reduce Hg^{2+} to less toxic volatile elemental mercury.

Metal interactions in *D. radiodurans* have been of interest not only from the point of view of metal detoxification/remediation but also due to the important role that certain heavy metals play in the radiation resistance physiology of this organism. *D. radiodurans* accumulates exceptionally high intracellular manganese and low iron levels. Accumulation of Mn^{2+} in deinococci is important for radiation resistant phenotype by facilitating recovery from radiation damage (Daly et al., 2004). It is believed that Fe-rich, Mn-poor cells are killed rapidly even at low radiation doses possibly due to the release of Fe^{2+} from proteins during irradiation, leading to cellular damage by Fe^{2+}-dependent oxidative stress. In contrast, Mn^{2+} ions concentrated in *D. radiodurans* might serve as antioxidants that reinforce enzymic systems which defend against oxidative stress during recovery (Ghosal et al., 2005).

Cadmium, an element with virtually no biological function, is a highly toxic metal. Cd^{2+} ions mediate their toxic effects by the induction of oxidative stress and also due to their strong affinity for –SH groups and ability to compete with other divalent metal ions for binding to proteins. The effect of this metal on radiation resistance in deinococci has not been well explored. For most of the genetic engineering as well as physiological studies, *D. radiodurans* has been the model organism. The present chapter deals with the comparison of heavy metal resistance/tolerance of *D. radiodurans* R1 (DR1) and other newly isolated strains of deinococci. A detailed study of effect of Cd^{2+} in relation to Mn^{2+} in various physiological responses is presented.

3.2 Materials and methods

3.2.1 Bacterial strains and plasmids

The bacterial strains and plasmids used in this study are described in Table 3.1. The deinococcal cultures were grown in TGY (0.5% tryptone; 0.1% glucose; 0.3% yeast extract). The *D. radiodurans* R1 (DR1) mutants carrying the kanamycin/ cholaramphenicol/hygromycin marker were cultured in the presence of 50 µg/ml kanamycin, 3 µg/ml cholaramphenicol, 25 µg/ml respectively. *E.coli* DH5α cultures

were grown at 37°C in Luria–Bertani (LB) broth or on LB agar. As per requirement *E.coli* DH5α was grown in L-B supplemented with ampillicin at a final concentration of 100 µg/ml (pTZ7R/T) and 50 µg/ml (pRADZ3). DR1 carrying pRADZ3 and its derivative were grown in TGY supplemented with 3 µg/ml cholaramphenicol.

3.2.2 DNA manipulations

Mini scale plasmid isolation from *E.coli,* restriction digestion and ligation were performed by the general protocols described by Sambrook and Russell, (2001). All the restriction enzymes were either procured from Bangalore genei Pvt. Ltd. (Bangalore, India) or MBI Fermentas (Germany). DR1 was transformed by the $CaCl_2$ method described by Satoh et al., (2009). Briefly, DR1 cells (1 ml) grown to early stationary phase (16 h of approx. 1.2 $OD_{600\ nm}$) were harvested by centrifugation, at 9650 g for 3 min., washed with 1 ml of TGY broth, resuspended in 0.1 ml of TGY broth, amended with 40 µl of 0.3 M $CaCl_2$. A 30 µl aliquot of the cell mixture and 10 µl of plasmid DNA (200–400 µg/µl) were mixed in a new culture tube and incubated at 30 °C for 90 min. To this 2 ml of TGY broth was added and the mixture was incubated at 30 °C for 24 h. The culture was appropriately diluted with 10 mM sodium phosphate buffer (pH 7.0) and spreaded on TGY plates supplemented with 3 µg /ml choloramphenicol. The transformants were scored after 3-5 days of incubation at 30 °C.

3.2.3 Influence of heavy metals on growth of radiation resistant bacteria

The heavy metal tolerance of the cultures was determined in TGY broth using a late logarithmic phase culture. TGY containing tubes were amended with different metals ($CdCl_2$, $HgCl_2$ and $K_2Cr_2O_7$) at concentrations mentioned and were inoculated at an initial OD_{600} of 0.1. The cultures were incubated at 30 °C under shaking condition for 12 h after which growth was recorded as OD_{600} measurements and expressed as percentage survival by considering the growth in media without any metal as 100 %. To study the growth phase dependence on metal tolerance, the cultures used for inoculum were grown to either late log phase, 12 h, or stationary phase, 48 h, inoculated at an initial OD_{600} of 0.1. To analyse the effect of Mn^{2+} on Cd^{2+} toxicity, 100 µM of Mn^{2+} was added to the media. Percentage survival was calculated as described.

3.2.4 Influence of Cd^{2+} and Mn^{2+} on recovery from H_2O_2 damage

Exponentially growing bacterial cultures were freshly inoculated in TGY broth at an OD_{600} of 0.1. Cultures were allowed to grow for 8 h and the OD_{600} was set to 0.6. H_2O_2 was added at a concentration of 20 mM. Aliquots were taken at different time intervals and appropriate dilutions were plated on TGY and TGY amended with 2.5 μM Cd^{2+} or 100 μM Mn^{2+}. Surviving fraction was enumerated after incubation for 48 h at 30 °C.

3.2.5 Influence of Cd^{2+} and Mn^{2+} on recovery from UV damage

The deinococcal cultures were grown to late exponential phase, washed with 0.8 % saline and OD_{600} adjusted to 0.4. The suspension (10 ml) was taken in sterile petri plate and irradiated in UV chamber with 254 nm UV source (Wilber Lourmat, France). Aliquots were withdrawn after exposing to UV doses of an increment of 200 J/m^2 and appropriate dilutions were plated on TGY and TGY amended with 2.5 μM Cd^{2+} or 100 μM Mn^{2+}. The colonies were enumerated after 72 h at 30 °C.

3.2.6 Determination of reactive oxygen species (ROS) in bacterial cells

Cells grown aerobically in TGY medium to an OD_{600} ~0.4 were exposed for 90 min to varying concentration of Cd^{2+} and H_2O_2. Cell suspensions were centrifuged, washed with 10 mM potassium phosphate buffer, pH 7.0, and incubated for 45 min in the same buffer containing 10 μM 2′,7′-dichlorodihydrofluorescein diacetate (H_2DCFDA), dissolved in dimethyl sulfoxide. Cells were subsequently washed and resuspended in 250 μl of 10 mM potassium phosphate buffer, pH 7.0 and disrupted by sonication (Perez et al., 2007). One hundred microliters of the resulting cell extracts were mixed with 1 ml of the same buffer and fluorescence intensity was determined using Thermo-Spectronic, Model F-7000 FL Spectrophotometer (excitation 490 nm, emission 519 nm). Emission values were normalized to protein concentration determined by Bradford's method (Bradford, 1976).

Table 3.1 Bacterial strains and plasmids used in the study.

Bacterial strain	Relevant information	Source/Reference
E.coli DH5α	*supE44 DlacU(t80lacZDM15) hsdR17 recA1 endA1 gyrA96 thi 1 relA1*	Laboratory stock
D. radiodurans R1 ATCC13939	Wild type	Prof. Mary Lidstrom, University of Washington, U.S.A.
Deinococcus sp. Grk2	Isolate from Greater Rann of Kutch, Gujarat, India.	This study, Chapter 2
*Deinococcus sp.*Grk4	Isolate from Greater Rann of Kutch, Gujarat, India.	This study, Chapter 2
Deinococcus sp. Grk5	Isolate from Greater Rann of Kutch, Gujarat, India.	This study, Chapter 2
D. radiodurans MD885, *sodA*⁻	R1 but *sod A:: aph*	Prof. M. J. Daly, Uniformed Services, University of the Health Sciences, Bethesda, U.S.A. Markillie et al., (1999)
D. radiodurans JAK1, *pprI*	R1 but *pprI536::aph*	Prof. I. Narumi, Japan Atomic Energy Agency. Ohba et al. (2005)
D. radiodurans XCSP1, *pprM*	R1 but *pprM286::hph*	Prof. I. Narumi, Japan Atomic Energy Agency, Ohba et al., (2009)
D. radiodurans TNK 106, *recA*⁻	R1 but *recA::cat*	Prof. John Battista, Louisiana State University Tanaka et al., (2004)

Plasmids

pRADZ3	Shuttle vector between *E.coli* and *D.radiodurans* R1, *groESL* promoter:: *lacZ* fragment of pMUTIN2mcs;10kb; *E.coli*(Amp^r) and Cat^r (DR1)	Prof. Mary Lidstrom, University of Washington, U.S.A. Meima and Lidstrom, (2000)
pTZR/T-*precA*	T-vector containing *rec*A promoter; Amp^r	This study
pRADZ3-*precA*	pRADZ3 with *precA* :: *lacZ* repoter	This study

aph: Kanamycin rsistance; *hph* : Hygromycin resistance; *cat*: cholramphenicol

3.2.7 Assay of reactive oxygen species (ROS) combatting enzymes

a) Superoxide dismutase (SOD)

SOD was analyzed using alkaline pyragallol method described by Marklund and Marklund, (1974). Briefly, 950 µl of 100 mM Tris-Cl (pH 8.0) was combined with 50 µl of 6 mM pyrogallol, prepared in 0.1M HCl. The initial OD was set to 0.03. An appropriate aliquot of the crude enzyme was added and inhibition of the auto-oxidation monitred. One unit of SOD was defined as the amount of enzyme that causes 50 % inhibition of the pyrogallol autooxidation rate at 420 nm. Protein concentration was determined by Bradford method (Bradford, 1976) for calculating specific activity.

b) Catalase

Catalase activity was measured spectrophotometrically by monitoring the decrease in absorbance at 240 nm due to decomposition of hydrogen peroxide in 100 mM potassium phosphate buffer, pH 7.0 at 25 °C. Breifly, 900 µl of 100mM potassium phosphate buffer, pH 7.0 was combined with 50 µl of 0.7 % H_2O_2 such that the initial OD is set at 0.4. An appropriate aliquot of crude extract was added and decrease in absorbance is recorded at an interval of 10s. One unit of the catalase was defined as the disappearance of 1 µmol of hydrogen peroxide ($\Sigma = 0.041\ mM^{-1}\ cm^{-1}$) (Yun and Lee, 2000). Protein concentration was determined by Bradford method (Bradford, 1976) for caliculating specific activity.

3.2.8 Activity staining of ROS reactive combative enzymes

c) Superoxide dismutase (SOD)

SOD activity staining done by method described by Yun and Lee, (2001). Briefly, proteins were resolved by 10 % nondenaturing polyacrylamide gel electrophoresis

(PAGE) in Tris-glycine buffer. The gels were soaked in 490 µM NBT for 20 min, then in a solution containing equal volumes of 28 mM TEMED, 28 µM riboflavin and 36 mM potassium phosphate buffer (pH 7.8) for 15 min. The gels were subsequently illuminated with a fluorescent lamp for 5-15 min to visualize white bands of SOD activity on the blue background.

d) Activity staining of Catalase

Proteins in cell-free extract were resolved by 10 % non-denaturing polyacrylamide gel electrophoresis (PAGE) in Tris-glycine buffer. Gels were incubated initially with 5 mM hydrogen peroxide followed by a freshly prepared mixture of 2 % ferric chloride and 2 % potassium ferric cyanide. Catalase bands were visible as yellow bands against a green background (Yun and Lee, 2000).

3.2.9 Construction of pRADZ3-PrecA

*rec*A promoter (P*rec*A) from *D. radiodurans* R1 was PCR amplified using the forward primer containing *Bgl*II site P*rec*AF: 5′-CATG*AGATCT*CCGGTTGCCGTAAAGCT-3′ (*Bgl*II underlined) and the reverse primer containing *Spe* I site P*rec*AR: 5′CTTC*ACTAGT*CCCCGTTCGCCCAGTTC-3′ (*Spe* I site underlined). PCR was carried out in 30 µl reaction mixture consisting of 1ng of DR1 genomic DNA, 30 pmole of each of the primers, 1 µl of mixture of dNTPs 2.5 mM each, 1.5U of Taq polymerase, combined with appropriate amount of 10X Taq polymerase buffer. Amplification was carried out in AB Biosystems thermal cycler (CA., USA). The PCR reaction was carried with an initial denaturation at 94 °C for 5 min.followed by 30 cycles each consisting of denaturation at 94 °C for 30 s., annealing at 50 °C for 30 s, elongation at 72 °C for 45 s, and a final extension at 72 °C for 10 min. The amplified products were analysed on 1 % agarose gel.

The amplified promoter was cloned in pTZ57R/T according to the manufacture's instruction (MBI Fermentas, Germany) and transformed in *E.coli* DH5α by $CaCl_2$ method described by Sambrook and Russell, (2001). For expression in DR1 the *rec A* promoter was sub cloned in the *Bgl*II and *Spe* I site of pRADZ3.

3.2.10 β-galactosidase assay

For quantitative analysis of *lac*Z expression, cells were permeabilized with Triton X-100 as follows. Samples (1 ml) of cultures at an OD_{600} 0.3 (or an equivalent volume) were centrifuged and the cell pellets were resuspended in 60 µl of lysis

buffer (10 mM Tris-HCl pH 8, 1 mM EDTA, 100 mM NaCl, 1.5 % SDS (w/v), 2.5 % Triton X-100) (v/v), (Bonacossa de Almeida et al., 2002). The suspension was incubated for 10 min at 0 °C before β-galactosidase was assayed as described by Miller, (1982). The activity of *lacZ* was determined using a molar absorption coefficient of 0.0045 $nmol^{-1}$ ml^{-1} cm^{-1} at 420 nm. The protein concentration was determined by Bradford method (Bradford, 1976) for estimating specific activity.

$$\beta\text{-galactosidase specific activity} = \frac{OD420 \times 1.7}{0.0045 \times t \times v}$$

where 1.7 ml is the total volume of the assay mixture; t is time (min); v= volume of cells taken for the assay i.e. 1ml.

3.2.11 Quantification of total carbonylated protein

The total carbonyl content in cellular proteins was determined spectrophotometrically as described by Semchyshyn et al., (2005). Crude extracts were prepared from *D. radiodurans* R1 cells treated or untreated with varied concentrations of Cd^{2+} for 12 h. Extracts were treated with streptomycin sulfate (2 %) and incubated on ice for 15 min. Precipitated nucleic acids were discarded by centrifugation at 14,000 g for 5 min. After adding four volumes of 10 mM dinitrophenylhydrazine (DNPH) prepared in 2 M HCl to 100 µl of the nucleic acid-free supernatant, the mixture was incubated for 1 h at room temperature with vortexing every 10–15 min. Proteins were precipitated by adding 500 µl of 20 % trichloroacetic acid (TCA) and then sedimented by centrifugation at 14,000 g for 5 min. The pellet was washed at least three times with an ethanol:ethylacetate mixture (1:1) to remove any unreacted DNPH and redissolved at 37 °C with 450 µl 6 M guanidine HCl. Carbonyl content was determined spectrophotometrically at 370 nm using a molar absorption coefficient of 22,000 M^{-1} cm^{-1}(Semchyshyn et al., 2005).

3.2.12 Immunodetection of carbonylated proteins

DNPH derivatized protein extracts prepared as described in Section 3.2.11 were analyzed by 12 % SDS-PAGE, using 25 µg of derivitised protein per lane. Gels were either stained with coomassie brilliant blue or transferred to nitrocellulose membrane filters using a tank blot system (Bangalore genei Pvt. Ltd., India). Electroblotting was done in a buffer system consisting of 25 mM Tris, 192 mM glycine, 10 % methanol at 50 V for 3 h. (Harper and Speicher, 2001). The transferred proteins were detected using 0.5 % Ponceau S (prepared in 5 % acetic acid). To detect the carbonylated

proteins anti-dinitrophenyl (anti-DNP) antibodies (Sigma, St. Louis, USA) were used. The membrane was blocked for 1 h at RT using 2 % skimmed milk prepared in phosphate buffered saline, (PBS) (137 mM NaCl, 2.7 mM NaCl, 100 mM Na_2HPO_4, 2 mM KH_2PO_4, pH 7.4). Immunodetection was done using mouse monoclonal anti-DNP antibodies at 1:5000 dilution for 1 h at RT. Unbound antibody was washed using 0.005 % Tween-20 in PBS by gently rocking the membrane for 1 min. This step was repeated thrice. Goat anti-mouse IgG- peroxidase conjugate (Bangalore Genei Pvt. Ltd., Bangalore, India) was used at 1:5000 dilution as secondary antibody. The excess of antibody was washed using 0.005 % Tween-20 in PBS. The carbonylated proteins were then detected by treating the membrane with 5 mg 3′,5′, di aminobenzidine (DAB) dissolved in 10 ml PBS containing 2 mg $NiCl_2$ and 10 µl 30 % H_2O_2 .The carbonylated protein appeared as brown bands (Gallagher, 2001).

3.2.13 Determination of thiobarbituric acid-reactive substances (TBARs)

TBARs in cell extracts were determined as described by Semchyshyn et al., (2005). The cultures of DR1 were grown in presence of varying concentration of Cd^{2+} in a volume of 600 ml for 12 h. The cells were collected by centrifugation at 9560 x g for 10 min, washed with 0.1 volumes of PBS, concentrated by centrifugation and resuspended in 0.05 volume of PBS. A 1ml aliquot of cell suspensions was treated with 1 ml of 20 % TCA (w/v) and centrifuged at 10,000 g for 5 min. Supernatants were mixed with 2.0 ml of a saturated solution containing thiobarbituric acid (0.67 %, w/v) prepared in 0.1 M HCl. Samples were then heated for 60 min in a water bath kept at 100 °C. Aliquots of 1.5 ml were then removed, chilled, mixed with 1.5 ml of butanol and centrifuged at 4,000 g for 10 min. The organic fraction was recovered and the OD_{535} was measured spectrophotometrically. TBARs content was determined using a molar extinction coefficient of 156 mM^{-1} cm^{-1} (Semchyshyn et al., 2005).

3.2.14 Metal binding protein preparation by Immobilised metal affinity chromatography (IMAC)

A 5 ml syringe (6.5 cm x 1.5 cm) was packed with glasswool to which 1 ml of the Imino diacetic acid (IDA- Agarose (Biorad Ltd, CA, USA) was pipetted using cut tips. The column was equilibrated with 5 column volumes of solution C (50 mM sodium acetate, 0.3 M NaCl, pH 4.0) and 5 column volumes of 0.3 M solution of either $MnCl_2$ or $CdCl_2$was applied to the column to charge the column of appropriate metal solution, while the control column was washed with equal volume of solution

C. The columns were washed with solution C to remove any excess of metal solution. The column was then washed with 10 column volumes of deionised water and allowed to equilibrate with at least 5 column volumes of solution A (50mM sodium phosphate, 0.3 M NaCl, pH 8) (Bio-rad, CA, USA).

DR1 cells grown in a volume of 600 ml at different conditions were harvested at 12,300 g for 10 min and frozen at -20 °C till used. The thawed cells were resuspended in 1:10 (w/v) in solution A and then disrupted using French press at 1000 psi. The suspension of disrupted cells was centrifuged at 12,300 g for 10 min. The supernatant was collected and was filtered using 0.45 µm filter. IDA-agarose column charged with appropriate metal was used for purification of the protein. Crude cell lysate (900 µg protein) was loaded on IDA-agarose column, washed with solution A till OD_{280nm} 0.001 was obtained. Elution of protein was done using 5 bed volumes of solution B (solution A + 500 mM Immidazole) at a flow rate of 1ml/min. Eluted protein fractions were resolved on 12 % SDS-PAGE and detected by silver staining (Sambrook and Russell, 2001). The gels were analysed using the online software, BIONUMERICS (Applied Maths, Belgium). The fractions containing maximum protein were pooled together and dialyzed for 24 h against 10 mM Tris-Cl pH 8.0. The samples were lyophilized and resuspended in minimum volume of distilled water.

The columns were recharged by washing with 10 bed volumes of eluting solution (solution A + 0.5 M EDTA) to strip the column from any adhering metal. Five bed volume of 1 M NaOH was used for rinsing the column to remove precipitated, hydrophobic and lipoproteins. The column was rinsed with distilled water till pH 7.0 was obtained. Washing was done with 10 bed volume of solution A.

3.2.15 Two- Dimensional gel electrophoresis (2-DE)

D. radiodurans cells grown in a volume of 600 ml at different conditions were harvested at 12,300 g for 10 min and frozen at -20 °C untill used. The thawed cells were resuspended in 1:10 (w/v) in Tris-buffered sucrose (10 mM Tris-Cl pH 7.0; 250 mM sucrose). Washed cells were disrupted using French press at 1000 psi. The cell lysate was briefly sonicated for 3 min (9.9 s on and 9.9 s off) to shred off DNA. The lysate was clarified by centrifugation at 12,300 g for 15 min at 4 °C and filtered through 0.45 µm membrane filter. The homogenates were treated with 10 µg/ml each of DNAase and RNAase, incubated at 4 °C for 12h. The samples were then dialysed against 1 mM Tris-Cl pH 7.0 for 3 h followed by concentration by lyophilisation. The

proteins were resuspended in 500 µL of distilled water.the protein concentration was estimated by Bradfords method (Bradford, 1976).

2-DE was performed according to the manufacturer's instruction (Bio-rad, CA, USA). Briefly, each protein sample,25 µg, in the lysis buffer was diluted to 125 µl with rehydration solution (9 M Urea, 2% CHAPS, 30 mM DTT, 0.5% ampholytes pH 3-10, 0.002% bromophenol blue). IEF dry strip gels (pH 4–7), 7 cm, (Bio-rad, CA, USA) were rehydrated with 125 µl of mixture solution in 7 cm strip holders and electrofocused with Protean (IEF) Isoelectric Focusing System (Bio-rad, CA, USA). The focusing protocol was performed as follows: 50 µA per strip at 20 °C; 250 V for 20 min; 4000 V for 2 h; and 15000 V/hr. After isoelectric focusing, strips were equilibrated (10 min) with gentle shaking in SDS equilibration buffer I (0.375 M Tris-HCl buffer, pH 8.8, 6 M urea, 20 % glycerol, 2 % SDS, 2 % DTT w/v), SDS equilibration buffer II (0.375M Tris-HCl buffer, pH 8.8, 6 M urea, 20 % glycerol, 2 % SDS, 2 % DTT, 2.5 % iodoacetamide w/v), then loaded onto SDS PAGE (12 %). The second dimension SDS electrophoresis was performed using Mini-PROTEAN SYSTEM. (Bio-rad, CA, USA). The protein spots were detected by silver staining (Sambrook and Russell, 2001) and the gels were compared using online 2D comparing software, Melanie 7.0 (Swiss Institute of Binformtics, Geneva, Switzerland).

3.3. Results and Discussion

3.3.1 Metal tolerance of radiation resistant bacteria

For the potential use of radiation resistant bacteria for the remediation of nuclear waste, the tolerance of the bacteria towards heavy metals, which are often accompanying the radionuclides in the dump areas, is important. The most common heavy metal contaminants at the radioactive waste sites are Cd^{2+}, Hg^{2+}, Cr^{6+} at varying concentration (NABIR Primer 3). Hence the tolerance of deinococci to the common metal contaminants was determined.

3.3.1a Tolerance to Hg^{2+}

The effect of Hg^{2+} was examined on the radiation resistant bacteria wherein the cultures showed varying level of sensitivty to Hg^{2+} (Fig. 3.1). DR1 exhibited extreme sensitivity to Hg^{2+} while the isolate Grk2 showed a maximum D_{50} of 2.08 µM, 2.3 fold higher than DR1. The highest reported concentration of Hg^{2+} at the radioactive waste sites is 10 µM (Lange et al., 1998). DR1 has been engineered to express the *mer*

A gene of *E. coli* BL308 and it results in tolerance upto 30 μM Hg^{2+} (Brim et al., 2000). *E. coli* shows a minimum inhibitory concentration (MIC) of 10 μM in minimal media (Nies et al., 1999) while *Ralstonia metallidurans* CH34 exhibits a MIC of 50 μM in minimal media (Dressler et al., 1991). Therefore DR1 is extremely sensitive to Hg^{2+} while Grk2 can be considered moderately resistant to Hg^{2+}.

3.3.1b Tolerance to Cr^{6+}

Chromium mainly occurs as Cr^{6+} in the divalent oxyanion chromate and as Cr^{3+}, the trivalent cation. Cr^{6+} which is more toxic than Cr^{3+} (Nies et al., 1999) is taken up by microbial cells as CrO_4^{2-} via sulfate (SO_4^{2-}) transport mechanisms (Silver and Phung, 2005). The Cr^{6+}tolerance of the radiation resistant bacteria revealed that DR1 showed a D_{50} upto 252 μM while the isolates showed considerably lower tolerance to Cr^{6+} (Fig. 3.2). The MIC of *E.coli* for Cr^{6+} has been reported to be 200 μM in minimal media (Nies et al., 1999). DR1 has been demonstrated to reduce Cr^{6+} with humic acid as final electron acceptor (Fredickson et al., 2000). Also complete mineralization of toluene by the bioengineered strain of DR1 with concomitant reduction of Cr^{6+} has been reported (Brim et al., 2006).

3.3.1c Tolerance to Cd^{2+}

Cadmium is also thiol-binding metal like Hg^{2+}. The toxic effects of Cd^{2+} is summed up under the general headings "thiol-binding and protein denaturation, interaction with calcium metabolism and membrane damage and interaction with zinc metabolism, or loss of a protective function" (Neis et al., 1999; Cuypers et al., 2010). Only in rare cases has an important single mechanism been found (Stohs and Bagchi, 1995; Cuypers et al, 2010). The deinococcal isolates and the type strain DR1 exhibited varying levels of tolerance, Grk2 being extremely sensitive to Cd^{2+} (Fig. 3.3). DR1 being moderately tolerant while Grk4 and Grk5 showed comparable tolerance. However, when compared to *E.coli* that shows a MIC of 500 μM; all the deinococcal strains can be considered sensitive to Cd^{2+} (Nies et al., 1999).

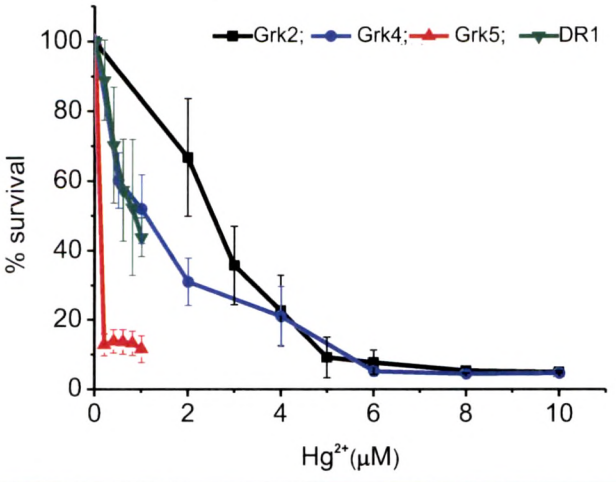

	D. radiodurans R1	Grk2	Grk4	Grk5
D_{50} (μM)	0.9 ±0.005	2.08± 0.59	1.23±0.34	0.078±0.26

Fig. 3.1: D50 determination of deinococcal strains to Hg^{2+}. D_{50} was determined as the concentration that results in the reduction in survival by 50 % of the control. Each point represents an average of three independent experiments. Table lists the D_{50} of all the isolates.

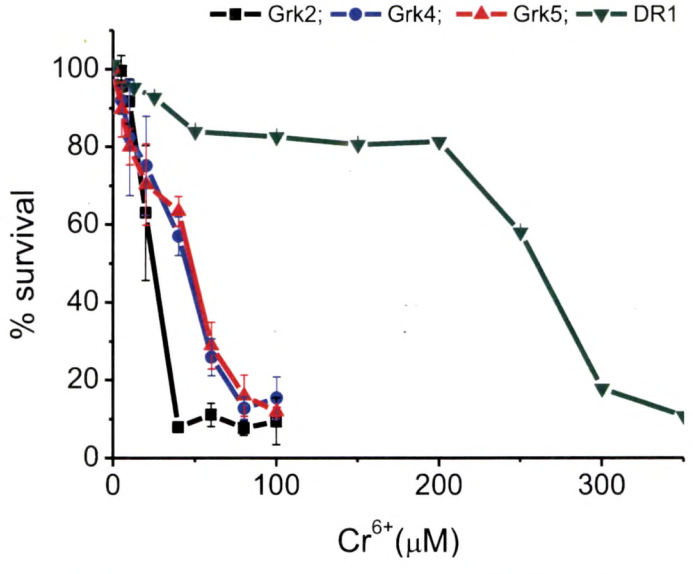

	D. radiodurans R1	Grk2	Grk4	Grk5
D_{50} (μM)	252.14±23	24.54±4.64	45.89±3.59	48.36 ±2.19

Fig. 3.2 D50 determination of deinococcal strains to Cr^{6+}. D_{50} was determined as the concentration that results in the reduction in survival by 50 % of the control. Each point represents an average of three independent experiments. Table lists the D_{50} of all the isolates.

Ruggerio et al., (2005) presented a comprehensive analysis of the effect of heavy metals and actinide on DR1 and *P. putida,* wherein they reported inhibitory concentration of 1.8 μM Cd^{2+} for DR1 while *P.putida* under similar condition could tolerate upto 500 μM. However both DR1 and *P. putida* showed comparable resistance to Cr^{6+} (Table 3.2).

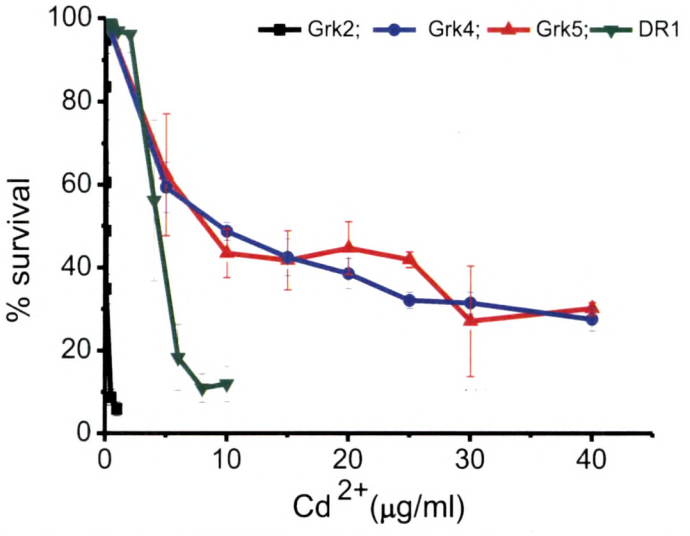

	D.radiodurans R1	Grk2	Grk4	Grk5
D_{50} (μg/ml)	3.91±0.36 (21)	0.076± 0.004 (0.41)	10.53± 0.37 (57)	9.48 ± 0.58 (51.7)

Fig. 3.3 D50 determination of deinococcal strains to Cd^{2+}. D_{50} was determined as the concentration that results in the reduction in survival by 50 % of the control. Each point represents an average of three independent experiments. Table below lists the D_{50} of all the isolates. Values indicated in parentheses represent the corresponding μM concentrations.

3.3.2 Effect of growth phases on Cd^{2+} toxicity

In nature, bacteria can survive for long periods in non-growing stationary states. Changes in morphology and physiology that occur in the stationary-phase bacteria and concomitantly a state of increased resistance against various stresses is established (Ishihama, 1999; Nystrom, 2004).

During the course of our work we observed the ability of DR1 to tolerate Cd^{2+} depended on the growth phase. Contrary to general observations, the exponentially growing cultures were able to tolerate higher concentration of Cd^{2+} as opposed to stationary phase culture when used as inocula in Cd^{2+} containing media (Fig. 3.4). In DR1, the log phase culture when inoculated in Cd^{2+} supplemented media, the culture did not show any growth inhibition, while the stationary phase inoculum was completely inhibited under the same Cd^{2+} concentration. The log phase culture grown in presence of Mn^{2+} exhibited Mn^{2+} induced cell division (MnCD), characteristic of DR1 (Chou and Tan, 1990). Growth in presence of Mn^{2+} and Cd^{2+} showed the dominant growth pattern of Mn^{2+} for log phase culture exhibiting a slight delay in MnCD effect, while Cd^{2+} growth pattern dominated for stationary phase culture. The Cd^{2+} D_{50} of exponential phase culture was determined to be 3.3 µg/ml whereas that of the stationary phase culture was 1.3 µg/ml (Fig. 3.5). The D_{50} value of Cd^{2+} in presence of Mn^{2+} increased and was comparable to log phase cells (Fig. 3.5). The exponential phase culture of DR1 did not show any stasis however, the stationary phase culture of DR1 underwent stasis of 48 h before resuming growth (Fig. 3.6).

Table 3.2 Comparative heavy metal resistance of radiation resistant bacteria, *E.coli* and *P.putida*

	Hg^{2+} (µM)	Cr^{6+} (µM)	Cd^{2+} (µM)	Reference
D. radiodurans R1	0.4	225	17 (3.28)	This study
Grk2	1.88	17.83	0.049 (0.009)	This study
Grk4	0.38	24.1	21 (3.9)	This study
Grk5	0.05	24.7	23 (4.34)	This study
E.coli[a]	10	200	500	Nies et al., (1999)
P.putida[b]	ND	100	530	Ruggerio et al., (2005)

† D_{70} values of deinococcal isolates for each of the metals are reported. The values in parentheses indicate the D_{70} for Cd^{2+} in µg/ml

[a] Refers to MIC determined in minimal media.

[b] Minimum concentration of metal that causes >70% growth inhibition.

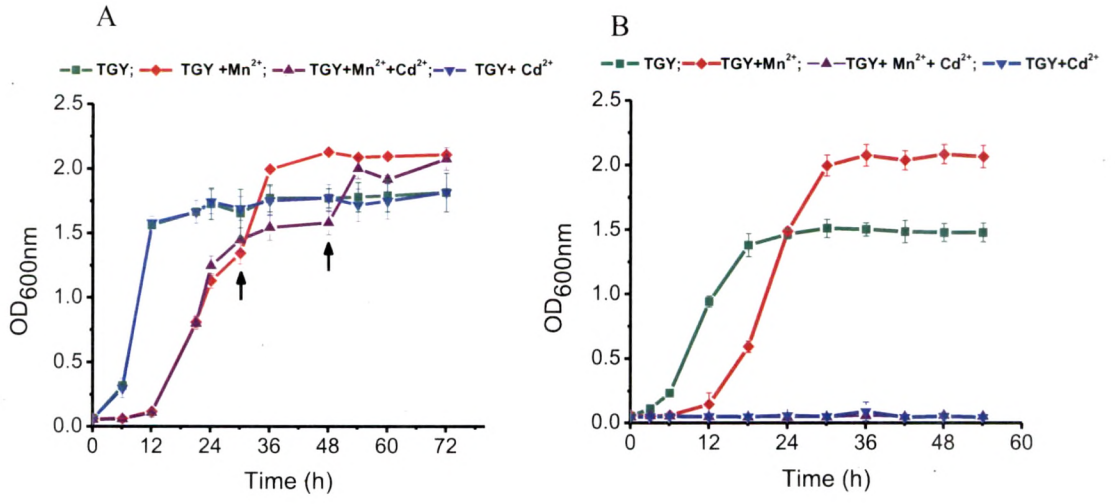

Fig. 3.4 Effect of growth phase on Cd^{2+} tolerance in DR1. The medium was supplemented with 1.2 µg/ml Cd^{2+}; 100 µM Mn^{2+} or both while no metal amendment served as control. A) Exponential phase; B) Stationary phase. Arrows indicate the MnCD effect.

Microscopic examination of the DR1cells 3 h post stasis, recovering from Cd^{2+} stress showed departure from the usual diplococci or tetracocci morphology of DR1, and exhibited lysed morphology. However the control cells showed the characterstic tetrad throughout the growth phase. After 6 h post recovery the cells exhibited diplococcic or teteracocci morphology but some unstained patches were observed in all the cells examined (Fig. 3.7), indicating cell envelop alterations. Ferianc et al., (1998) reported the lag phase cultures of *E.coli* could tolerate up to 3 µM Cd^{2+} with complete growth inhibition at 10 µM Cd^{2+} in minimal media as opposed to exponential phase culture that could tolerate up to 273 µM Cd^{2+}. Similarly log phase cultures of DR1 are 2.5 fold more resistant to Cd^{2+} than the stationary phase cultures.

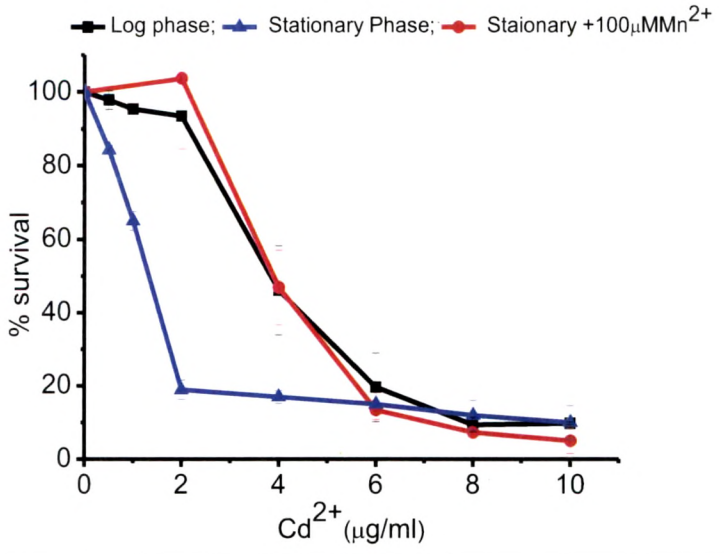

	DR1 log phase	DR1 Stationary phase	DR1 Stationary phase + 100 μM Mn^{2+}
D_{50} (μg/ml)	3.9± 0.36(21)	1.21±0.02 (6.6)	3.8±0.48(20)

Fig. 3.5 Effect of exogenous Mn^{2+} addition to Cd^{2+} toxicity to stationary phase cultures in DR1. Table below indicate the D_{50} value of DR1 under different growth conditions.

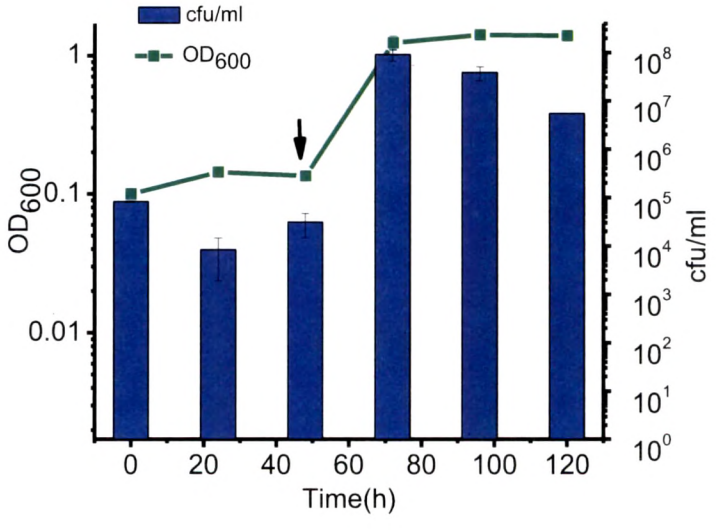

Fig. 3.6 Cd^{2+} induced stasis of the stationary phase culture of DR1. Arrow indicates the point of growth resumption

DR1 has been shown to accumulate Mn^{2+} intracellularly which protects the important biomolecules from lethal effects of ionising radiation (Ghosal et al., 2005). In several gram positive bacteria Cd^{2+} toxicity has been affected through Mn^{2+} transporters and are potent inhibitors for Mn^{2+} transporters (Hao et al., 1999; Makui et al., 2000; Keheres et al., 2000; Horsburgh et al., 2002). DR1 has two forms of Mn^{2+} transporters, Nramp Mn^{2+} transporters similar to the *mnt*H transporters identified in *E.oli* and *S. typhimurium* and ABC type transporters (Daly et al., 2004). The enhanced tolerance of Cd^{2+} in stationary phase culture of DR1 in presence of Mn^{2+} (Fig. 3.5) indicates that Cd^{2+} proves to be a competitive substrate for the Mn^{2+} transporters in DR1. An increased tolerance towards Cd^{2+} also affirms that Mn^{2+} ions are able to antagonize the transport of Cd^{2+}.

As opposed to the exponentially growing cultures of *E.coli* that undergo stasis when challenged with Cd^{2+} stress (Ferianc et al., 1998), stationary phase cultures of DR1 exhibited stasis (Fig. 3.6). In congruence with *E. coli* cultures, that require synthesis of new proteins for recovery after exposure to Cd^{2+} (Mitra, 1984). DR1 cells treated with cholaramphenicol failed to recover from Cd^{2+} induced statsis (data not shown). This affirms the fact that DR1 requires new protein synthesis to recover from stasis induced by Cd^{2+}. Additionally transcriptomic analysis of *E.coli* cells exposed to Cd^{2+} revealed down regulation of several ribosomal proteins. All genes for protein translation machinery are down-regulated, after which some resumed expression in the late phase, while genes for stress proteins were mostly up-regulated consistent with the decline in the overall rate of protein synthesis (Wang et al., 2005).

A

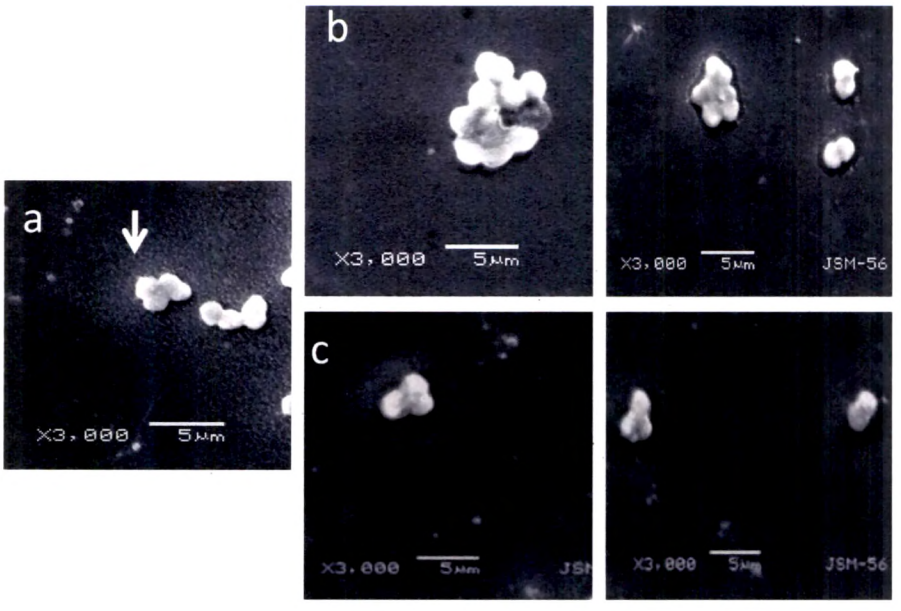

B

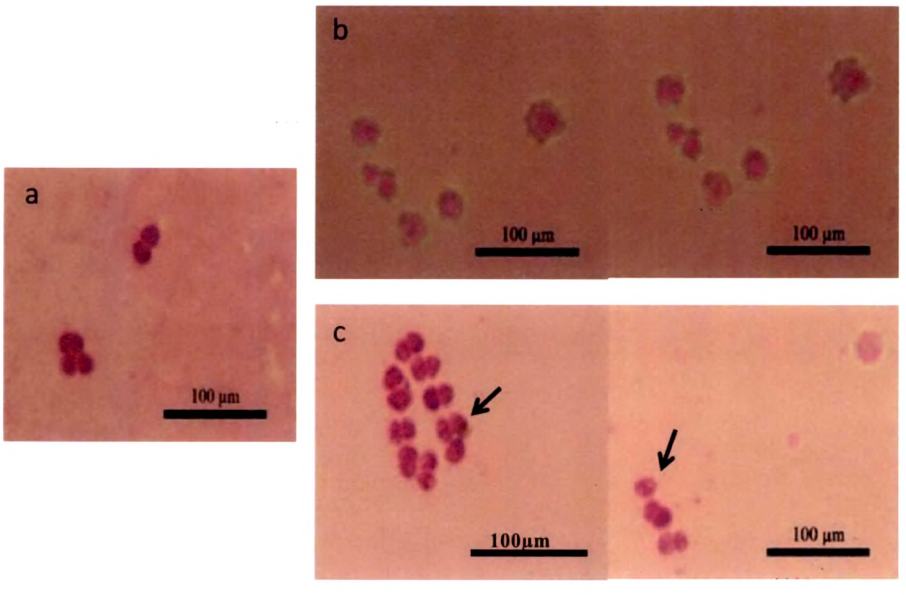

Fig. 3.7: Micrographs of the Cd^{2+} treated DR1 after assuming growth A) Scanning electron microscopy; B) Light microscopy of gram stained DR1; a) Control, the arrow shows normal tetrad of the DR1; b) 3 h post stasis; c) 6 h post stasis. The arrow represents the unstained patches on the cells.

Heavy metals such as Cu^{2+}, Co^{2+}, Hg^{2+} and Cd^{2+} are known to induce morphological changes leading to change in cell elongation (Chakarvarty and Banerjee, 2008; Antony et al., 2011; White and Gadd, 1998; El-Rab et al., 2006). However at higher concentrations, Co^{2+} and Hg^{2+} cause lysis of the cells (Vaituzis et al., 1975, Antony et al., 2011). Fig. 3.7 demonstrates that Cd^{2+} also affects morphological changes in recovering cells of DR1. Massalki et al., (1981) demonstrated that the cells of the green alga *Ankistrodesmus braunii* when exposed to Cd^{2+} showed the presence of multinucleate gaint cells formed due to continuous mitotic division without subsequent cytokinesis. The nuclei of such giant cells exhibited the presence of deep indentations that appeared hole like structures. Similar structures were also observed in DR1 cells that did not exhibit normal morphology (Fig. 3.8b). Recently, Joe et al., (2011) studied the transcriptional profile of DR1 exposed to toxic levels of Cd^{2+}. Among other genes, there was a down regulation of the expression of genes involved in biosynthesis of murein sacculus, surface polysaccharides, lipopolysaccharides and surface structures.

3.3.3a Cd^{2+} and reactive oxygen species (ROS) generation

Chemically reduced and acetylated 2′, 7′-dichloro hydrofluorescein diacetate (H_2DCFDA) is a non fluorescent dye that is freely permeable to the cells. Once inside the cells, it is hydrolysed to 2′, 7′ dichlorofluoroscein (DCF) and trapped intracellularly, DCF is then able to interact with peroxides resulting in fluorescent, 2′, 7′-dichlorohydrofluorescein.The fluorescent probe H_2DCFDA was used to monitor formation of intracellular ROS in Cd^{2+} treated cells of DR1 (Fig. 3.8). Cd^{2+} induces oxidative stress at sub-lethal concentration, however there is a decrease in intra-cellular ROS at D_{50} concentration of Cd^{2+} that can be attributed to increased lethality by increasing Cd^{2+} concentration (Fig. 3.9 (A)). A similar effect was seen with H_2O_2 wherein sub-lethal concentration elicits intracellular ROS that declines at higher concentration of H_2O_2 known to be lethal in DR1 Fig. 3.9 (B) (Wang and Schellorn, 1995). The ROS produced by 10 μM Cd^{2+} was similar to that produce by 60 mM H_2O_2 (Fig. 3.10).

Metal catalyzed oxidation and generation of oxidative stress *in vivo* is a commonly observed phenomenon for redox-active metals such as Fe^{2+} and Cu^{2+}. Although Cd^{2+} is considered to be a redox inactive metal, yet it has been shown to cause protein carbonylation a common index for the ROS induced damage (Stohs and Bagchi,

1995; Cuypers et al., 2010). The Cd^{2+} induced ROS demonstrated here could be a direct effect of Cd^{2+} or indirect by replacement of Fe from Fe-S cluster that can promote further Fenton type chemistry producing hydroxyl radical (Cuypers et al., 2010).

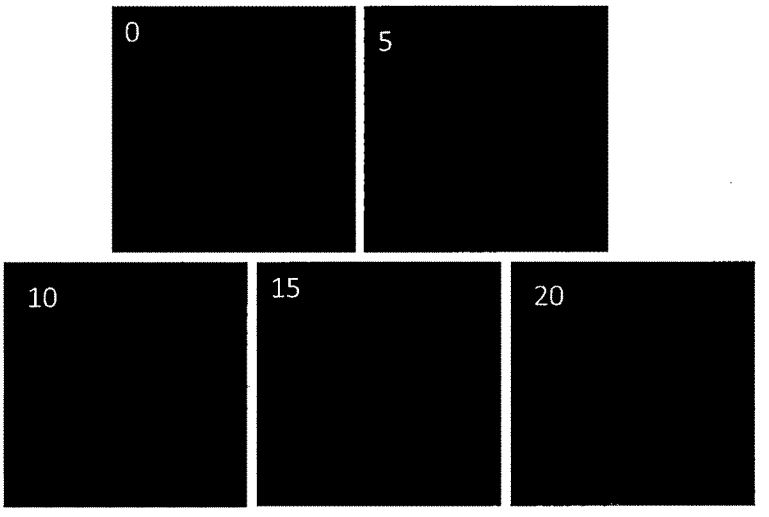

Fig. 3.8 Fluoresence micrograph of Cd^{2+} exposed DR1 cells stained with H2DCFDA. Numbers indicated are the Cd^{2+} concentration in μM

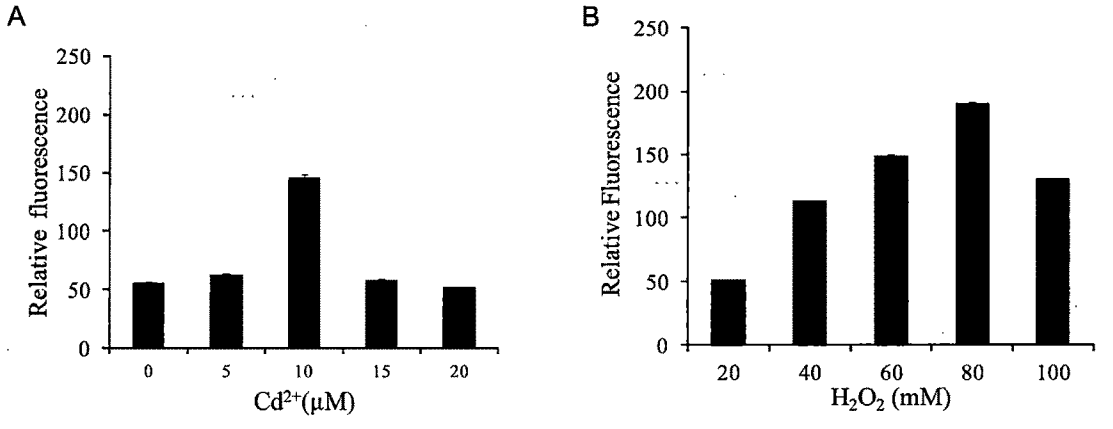

Fig. 3.9 Effect of Cd^{2+} and H_2O_2 on ROS generation in DR1. Relative fluorescence obtained by H_2DCFDA treated cells A) after Cd^{2+} treatment, B) after H_2O_2 treatment. Fluorescence obtained was normalised using the protein content after each treatment to obtain relative fluorescence.

3.3.3b Induction of protien carbonylation by Cd^{2+}

ROS has multiple targets in the cell with all biomolecules being affected by it (Imaly, 2003; Avery, 2011). Protein carbonyl derivatives are formed by direct metal

catalyzed oxidative (MCO) attack on the amino-acid side chains of proline, arginine, lysine, and threonine (Nystrom, 2005). The carbonylation of the protein renders the proteins inactive and more susceptible to degradation. In DR1, the protein carbonylation increased with increasing Cd^{2+} concentration which is congruence with the ROS that is produced (Fig. 3.10). However, a decrease in ROS activity at higher concentration but sustained levels of carbonylated protein was observed indicating that at higher concentrations Cd^{2+} may impair the degradative capacity of DR1. Immunoblot assay also reveals protein oxidation increases with increasing Cd^{2+} concentration (Fig. 3.11). Although the ROS declines beyond 10 μ M Cd^{2+} there is sustained presence of carbonylated proteins. A diminished degradative capacity of the cell may contribute to the persistence carbonylated protein in the cell (Nystrom, 2005).

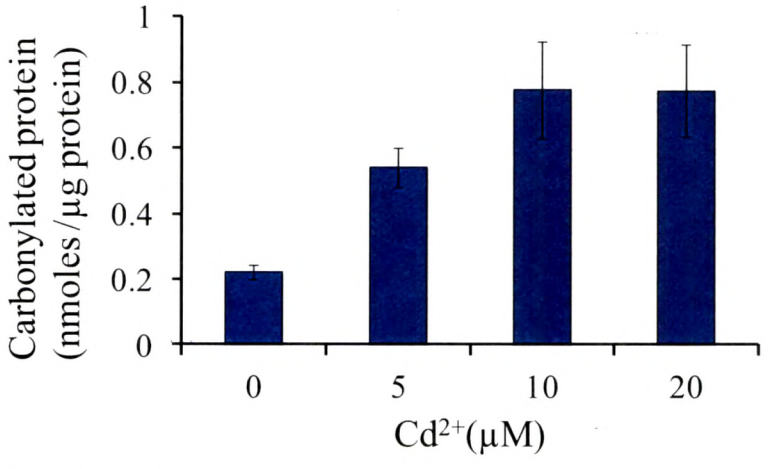

Fig. 3.10 Effect of Cd^{2+} on carbonylated proteins in DR1

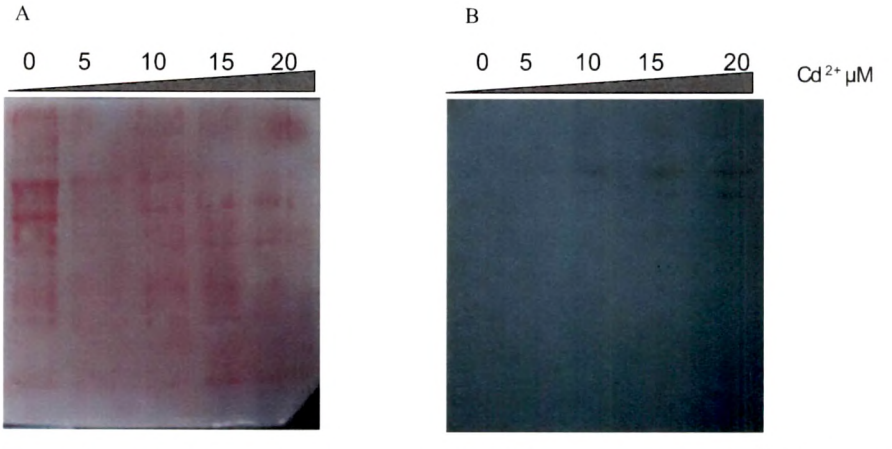

Fig. 3.11 Detection of carbonylated proteins in DR1 exposed to Cd^{2+}. A) Total cellular protein detection using Ponceau S; B) Immunodetection of carbonylated proteins by anti-DNP antibody.

3.3.3c Effect of Cd^{2+} on lipid peroxidation

Peroxidation of membrane lipids is a complex process involving unsaturated fatty acids and in particular, polyunsaturated fatty acids containing more than one methylene groups which are highly reactive to oxidizing agents. The oxidation can form peroxyl radicals that can set off a free radical chain reaction to other methylene groups and generate peroxidation by-products which could promote the loss of integrity in the plasma membrane and, eventually, lead to cell death (Perez et al., 2007). In DR1, Cd^{2+} induced the formation of lipid hydroperoxides, detected as TBARs, at all concentrations tested with a maxima obtained at 10μM (Fig. 3.12).

The TBARs detect primarily products arising from the decomposition of lipid hydroperoxides and is a common method to assess the damage to the lipids caused by free radicals (Howlett and Avery, 1997). Metals that promote Fenton type chemistry such as Cu^{2+} and H_2O_2 cause lipid peroxidation (Perez et al., 2007; Semchyshyn et al., 2005; Howlett and Avery; 1997). Howlett and Avery, (1997) demonstrated the lipid composition influenced the degree of lipid peroxidation with unsaturated fatty acids being more susceptible for lipid peroxidation. Fig. 3.12 demonstrates lipid peroxidation in DR1 which is in correlation with ROS production. The lipid peroxidation due to Cd^{2+} was not dose dependent, a similar effect was reported in *Allium cepa* and *Vicia fabia* followed by Cd^{2+} exposure (Unyayar et al., 2006).

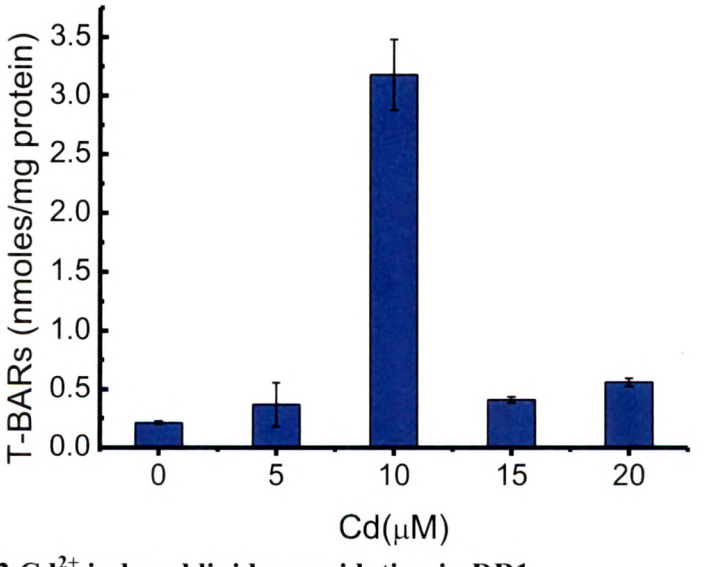

Fig. 3.12 Cd^{2+} induced lipid peroxidation in DR1

3.3.4 Effect of Mn^{2+} and Cd^{2+} on recovery from H_2O_2 stress in DR1

During starvation genes encoding proteins with specific roles in protecting the cell against external stresses, e.g., heat, oxidants, osmotic challenge, and exposure to toxic chemicals are expressed and these are the likely candidates required for starvation survival (Nystrom, 1999; Ishihama, 1997). Consequently, starved cells are highly resistant to a variety of secondary stresses, a phenomenon known as stasis-induced cross protection (Nystrom, 2004). It was hypothesised that inability of DR1 to tolerate Cd^{2+} in the stationary phase was due to the overwhelming oxidative stress that was produced by Cd^{2+}. Therefore we analysed the effect of Mn^{2+} and Cd^{2+} on cells recovering from oxidative stress imposed by treating the exponentially growing cultures to 20 mM H_2O_2 for different time intervals. As seen in Fig. 3.13 (A) pre-treatment of H_2O_2 enhanced the survivability of the DR1 culture in presence of Cd^{2+} indicating the cross-resistance provided by H_2O_2 to Cd^{2+} stress. However as seen in Fig. 3.13(B), pre treatment of Cd^{2+} was unable to provide any cross-resistance to H_2O_2 exposed cells while Mn^{2+} exhibited adaptability to either stress. To investigate the potential role of SOD in Cd^{2+} toxicity in DR1, *sod* A$^-$ (Mn SOD) disruptant mutant of DR1 was subjected to Cd^{2+} stress. The mutants were found to be 5 times as sensitive to Cd^{2+} as compared to wild type, while Mn^{2+} amendment to *sod* A$^-$ further aggravated Cd^{2+} toxicity (Fig. 3.14) which is in contrast to that observed for wild type (Fig. 3.15). Addition of Mn^{2+} to DR1cells demonstrates high SOD as well as catalase activity indicating the ROS stress (Chou and Tan, 2000). Furthermore addition of Mn^{2+} induces the Embden-Merenhof pathway (EMP) as opposed to the Pentose Phosphate pathway (PP) leading to massive glucose oxidation that creates oxidative stress and exhaustion of the reducing power of the cell (Zhang et al., 2005). This might explain the higher catalase and superoxide dismutase (SOD) requirement after exposure to high levels of Mn^{2+} as well as the higher sensitivity of sod A$^-$ mutant to Cd^{2+} in presence of Mn^{2+}.

3.3.5 Growth phase dependent production and influence of Cd^{2+} on anti-oxidative enzymes

The normal metabolism of aerobic cells also contributes to the ROS that is efficiently controlled by ROS combative enzymes produced by the cells (Imlay, 2003). The time course for the expression of catalase and SOD in DR1 under normal growth conditions was investigated. SOD activity was in good agreement to the values

reported for by Chou and Tan (1990) and the activity increased throughout the growth phase while showing a reduction of 75 % of the maximium activity obtained at 12 h, which was still 38 % greater than early log phase (Fig. 3.16 A). The catalase activity at 12 h, late exponential phase increased 10 fold as compared to the early exponential phase and decreased to the initial levels at early stationary phase. (Fig. 3.16 B)

The role of the two key anti-oxidative enzymes catalase and superoxide dismutase (SOD) toward Cd^{2+} toxicity was studied. Catalase was strongly inhibited even at the lowest concentration examined, 5 µM, showing a decrease of 80 % activity in comparision to control and was further corroborated by the activity staining (Fig. 3.17) .The observation is supported by the fact the constitutive catalase in DR1 is Kat A, heme –containing enzyme that may be inactivated by the presence of the Cd^{2+} (Kobayashi et al., 2006).

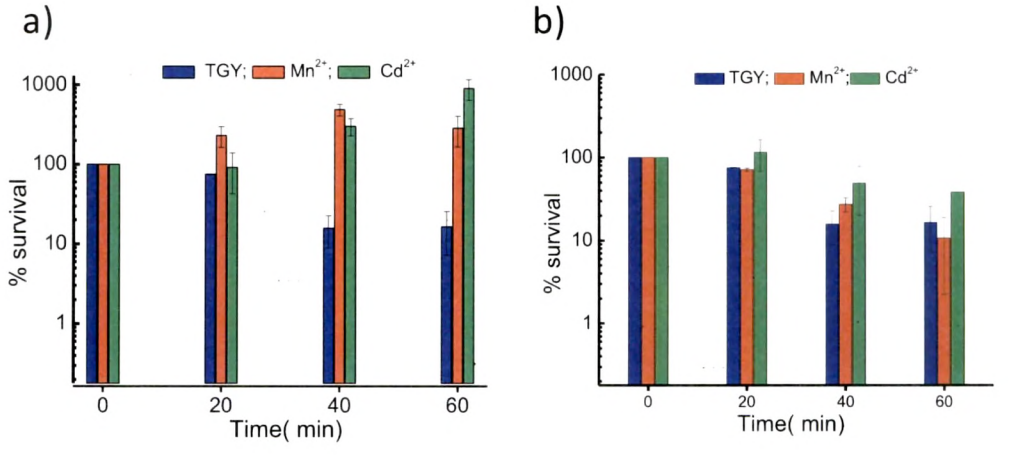

Fig. 3.13 Effect of Mn^{2+} and Cd^{2+} on recovery of DR1 from H_2O_2 A) cells are exposed to 20 mM H_2O_2 followed by recovery on TGY or TGY+100 µM Mn^{2+} or TGY+ 2.5 µM Cd^{2+}; B) Cultures are grown in TGY or TGY+100 µM Mn^{2+} or TGY+ 2.5 µM Cd^{2+}, exposed to 20 mM H_2O_2 followed by recovery on TGY plates.

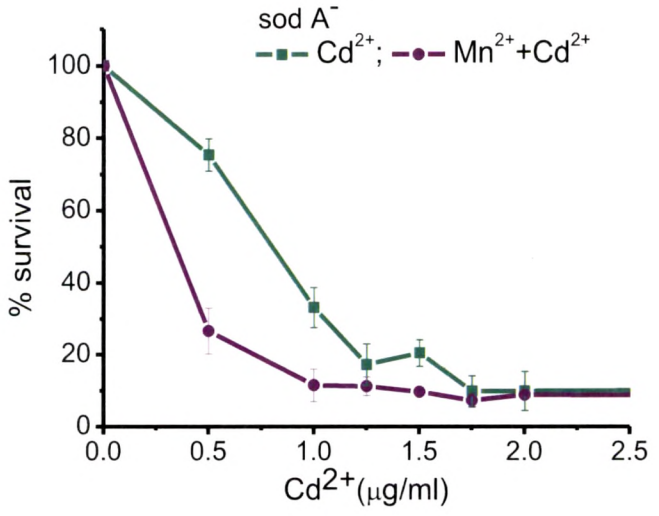

Fig. 3.14 Effect of Cd^{2+} on DR1 sod A^- mutant in presence and absence on 100μM Mn^{2+}.

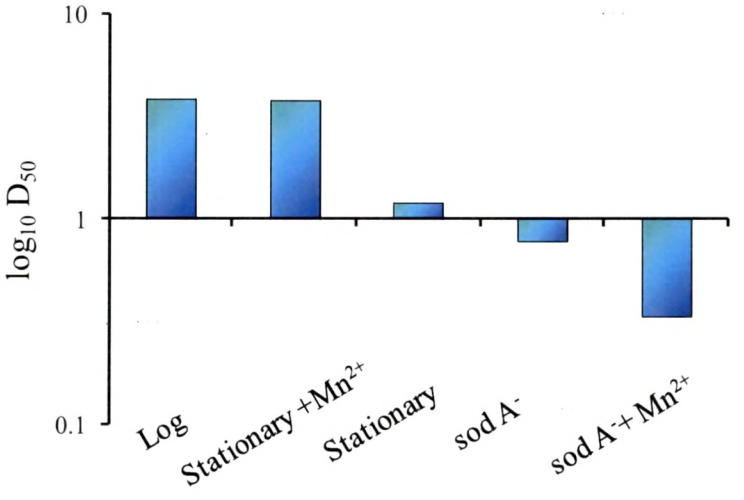

Fig. 3.15 A comparative analysis of Cd^{2+} D50 for the wild type DR1 grown under different growth phases and the DR1 sod A- mutant. The influence of Mn^{2+} on D_{50} for Cd^{2+} has been compared for both wild type and sod A^- mutant.

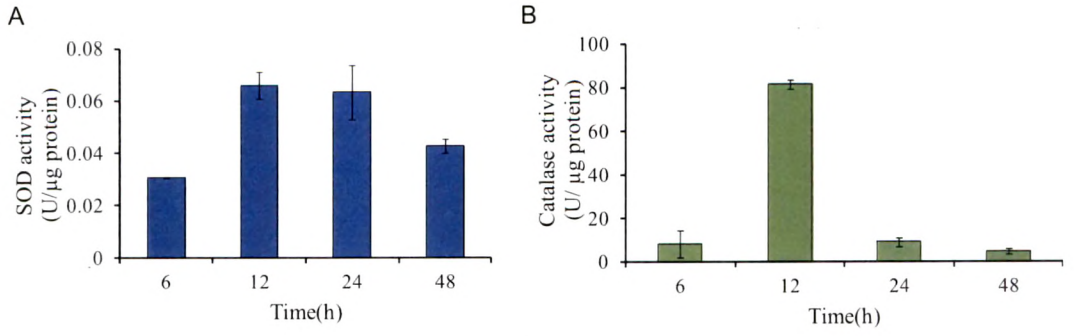

Fig. 3.16 Growth dependent expression of anti-oxidant enzymes in DR1 grown in TGY A) SOD; B) Catalase

No significant effect of Cd^{2+} on SOD activity was observed in the zymogram (Fig. 3.18 A). Nevertheless, activity measurements revealed a decline in the SOD activity at 5 µM Cd^{2+} and a complete inhibition at higher concentrations of Cd^{2+} treatment (Fig. 3.18 B). The *in vitro* effect of the Cd^{2+} on SOD enzynme activity from the Cd^{2+} untreated culture of DR1 showed that Cd^{2+} inhibited SOD activity by 10 % at 1 µM and 5 µM , while at 10 µM , 24 % reduction in the activity was observed.

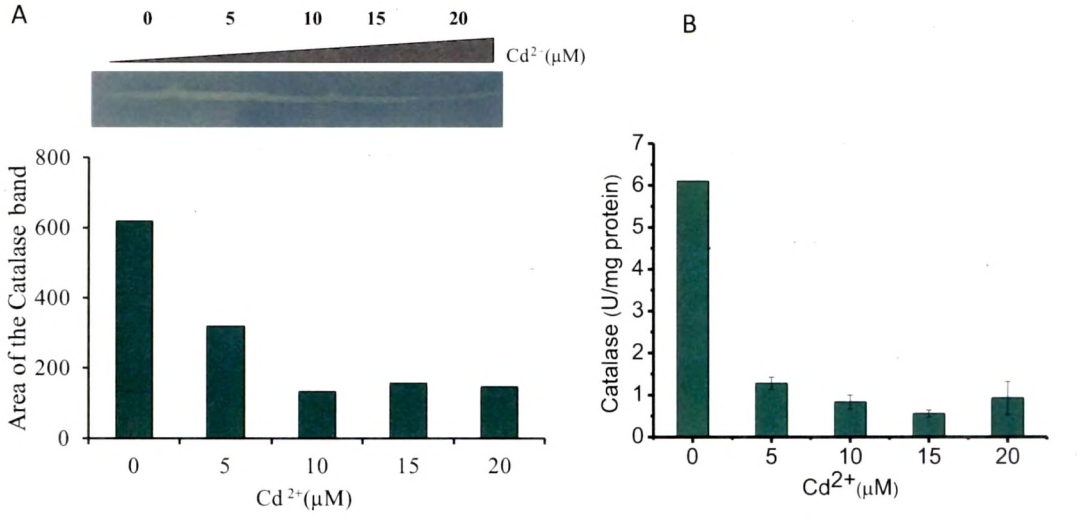

Fig. 3.17 Effect of Cd^{2+} on the catalase in DR1 A) Catalase zymogram and its densitometric scan; B) Activity of catalase in crude extract of DR1

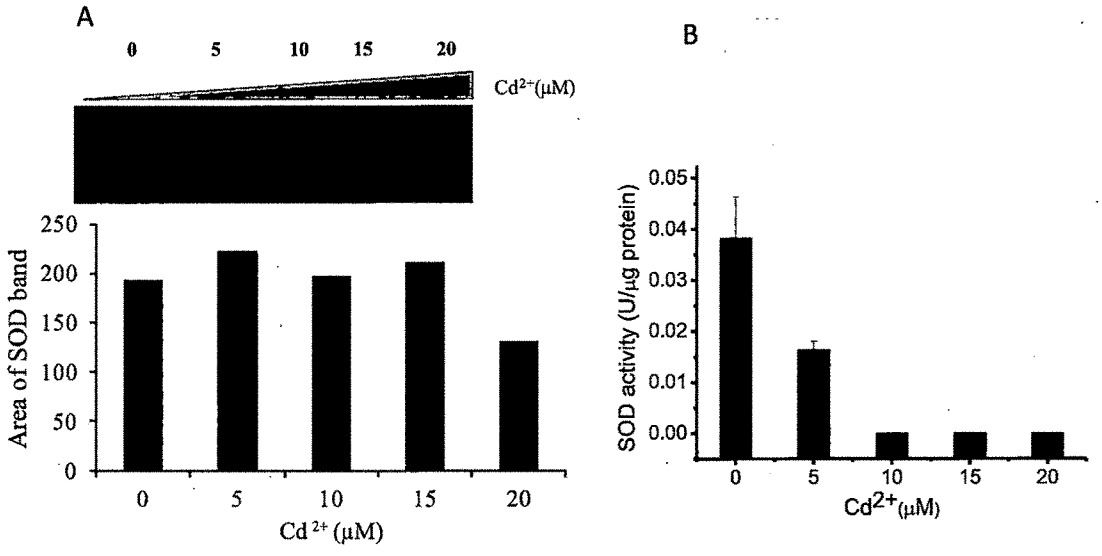

Fig. 3.18 Effect of Cd^{2+} on the SOD in DR1 A) SOD zymogram and its densitometric scan ; B) Activity of SOD in crude extract of DR1

3.3.6 Effect of Mn^{2+} and Cd^{2+} on survival after UV exposure

To analyze if UV damage could provide any cross resistance to the cells recovering in presence of Cd^{2+}, DR1 cells were exposed to UV and subsequently plated on Cd^{2+} containing plates. An enhanced survival of the cells recovering in presence of Cd^{2+}, amounting to about 1.37 times of the control, was observed which can be attributed to induction of the *uvr* genes and *rec* A for the repair of UV induced damage (Fig. 3. 19). Effect of Cd^{2+}on *rec* A$^-$ mutant, TNK106 was examined. The *rec*A$^-$ disruptant mutant, TNK106, proved to be more sensitive to Cd^{2+} while in presence of Mn^{2+}, Cd^{2+} toxicity seemed not to be significantly affected (Fig. 3.20). The *rec* A mutant demonstrated a D_{50} value of 0.925μg/ml (5.04 μM), while the wild type strain has a D_{50} value of 3.9 μg/ml (21 μM) which amounted to 4 fold sensitivity of the rec A mutant (Fig. 3.21). Direct role of homologous recombination for removal of UV photoproducts from genomic DNA DR1 has been reported (Tanaka et al., 2005). Our results are in accordance to the fact that UV induced recA in DR1 can facilitate enhanced recovery in presence of Cd^{2+}. The cells growing on TGY medium accumulate high levels of metabolic intermediates, which are necessary for DNA repair. The induction of an EMP pathway by Mn^{2+} deplete G-6-P and thus the the precursors for the nucleotide syntheisis. (Zhang et al., 2003). This explains the increase in UV sensitivities of TGY+Mn^{2+} recovered cells.

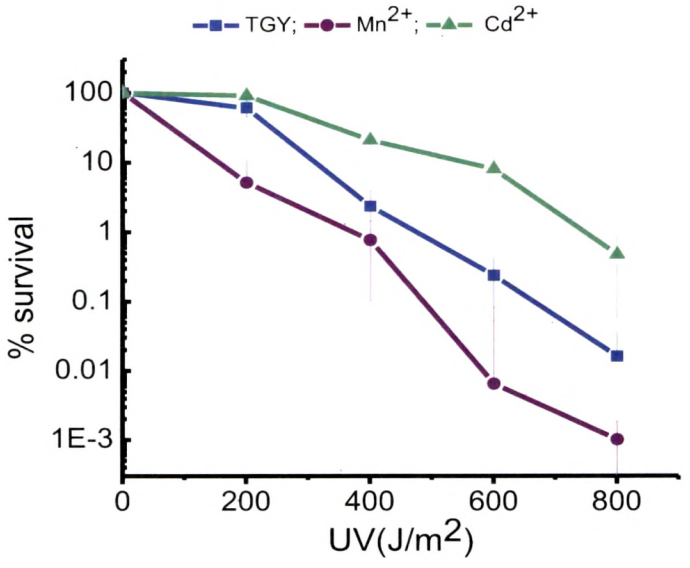

Fig. 3.19 Effect of Cd^{2+} and Mn^{2+} on recovery of DR1 from UV radiation.
The recovery was observed on TGY or TGY+100μM Mn^{2+} or TGY+ 2.5 μM Cd^{2+}

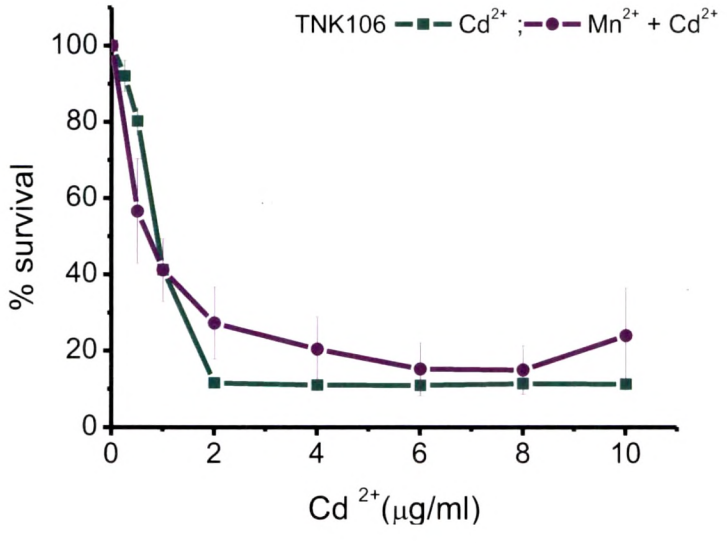

Fig. 3.20 Effect of Cd^{2+} on *rec* A⁻ mutant of DR1 in presence and absence of 100 μM Mn^{2+}

To assay if Cd^{2+} affects the expression of *rec*A in DR1, we created translational fusion of the *rec*A promoter of DR1 to *lac* Z reporter gene by the PCR amplification of *rec* A promoter (P*rec* A) of DR1 as 400 bp fragment from genomic DNA using specific primers (Fig. 3.22 A), and cloning of the same in pTZ57R/T.

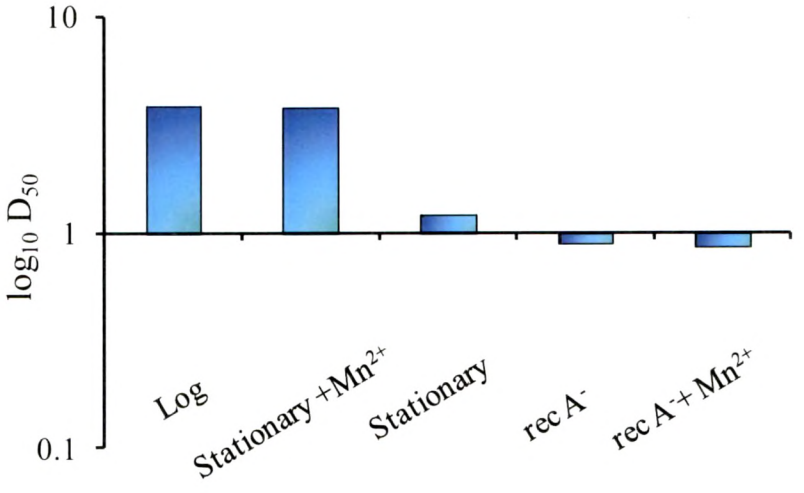

Fig. 3.21 A comparative analysis of Cd^{2+} D50 for the wild type DR1 grown under different growth phases and the rec A- mutant. The influence of Mn^{2+} on D_{50} for Cd^{2+} has been compared for both the wild type and the *rec* A⁻ mutant.

The pTZ57R/T clones were confirmed using promoter specific restriction enzymes, *Spe* I and *Bam* HI (Fig. 3.22 B) and amplification using promoter specific primers (Fig. 3.22 C). *gro*EL promoter from pRADZ3 was excised as a *Spe* I and *Bam* HI fragment followed by sub-cloning of recA promoter in *Spe* I and *Bam* HI site of pRADZ3. The clones obtained in *E.coli* DH5α were confirmed using *Spe* I and *Bam* HI and PCR amplification of the cloned fragment (Fig. 3.23). The confirmed plasmid, Prec A - pRAD Z3 (Fig. 3.24) was transformed in DR1 to obtain DR1 (Prec A - pRAD 4Z3).

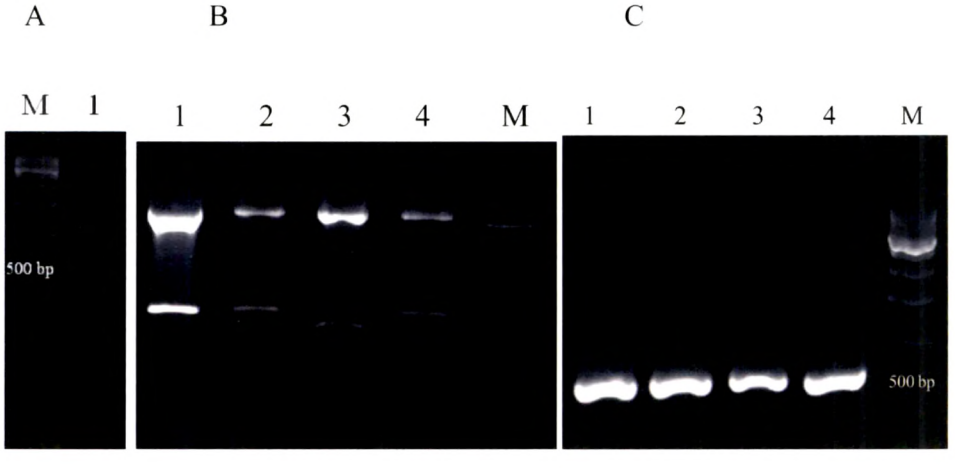

Fig. 3.22 Amplification and clone confirmation of the pTZ57R/T- A) amplification of PrecA from DR1 genomic DNA; B) Clone confirmation using *Spe* I

and *Bam* HI; C) PCR amplification. from the clones Lane 1: 8T-PrecA; Lane 2: 9T-PrecA; Lane 3: 16T-PrecA; Lane 4:20T-PrecA; M: 500 bp marker. Clone 8T-PrecA was used for further sub-cloning in pRADZ3.

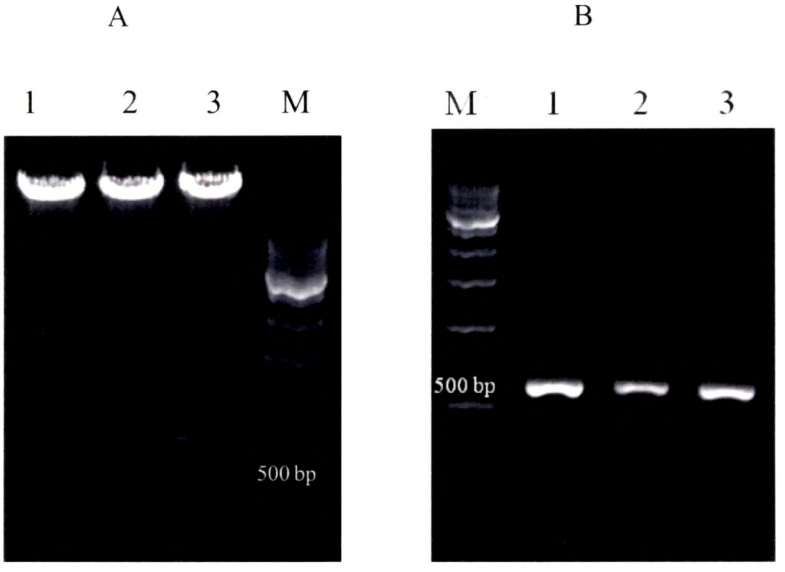

Fig. 3.23 Clone confirmation of the Prec A - pRAD Z3clones using. A) *Spe* I and *Bam* HI; B) PCR amplification. Lane 1: PrecA- 4Z3-; Lane 2: PrecA-7Z3; Lane 3: PrecA- 10Z3; M: 500bp marker. PrecA- 4Z3 was selected for transformation in DR1.

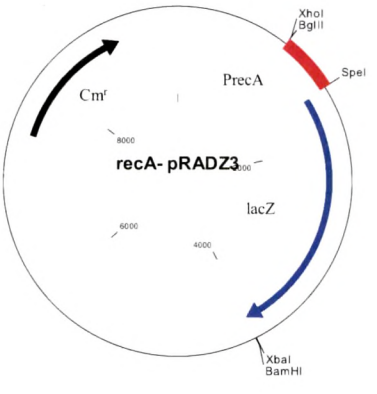

Fig. 3.24 Vector map of Prec A -pRAD Z3.

The effect of Cd^{2+} appears immediately as evident from increased activity at the onset. There was a dose dependent increase of the *lac* Z activity, however the activity decreased with prolonged incubation (Fig. 3.25). Min et al., (1999), created a *rec*A operator-promoter *luxCDABE* fusion to demonstrate the induction of *rec* A activity on

exposure to several mutagenic agents in *E.coli*. The authors demonstrated the dose dependent enhancement of the *rec*A activity on Cd $^{2+}$ exposure. The *rec*A promoter was upregulated in presence of Cd^{2+} in DR1, however prolonged incubation diminished the effect. The results are in agreement that Cd^{2+} induces the *rec*A activity indicating the possibility of the DNA damage although it cannot be stated if the effect is direct or indirect.

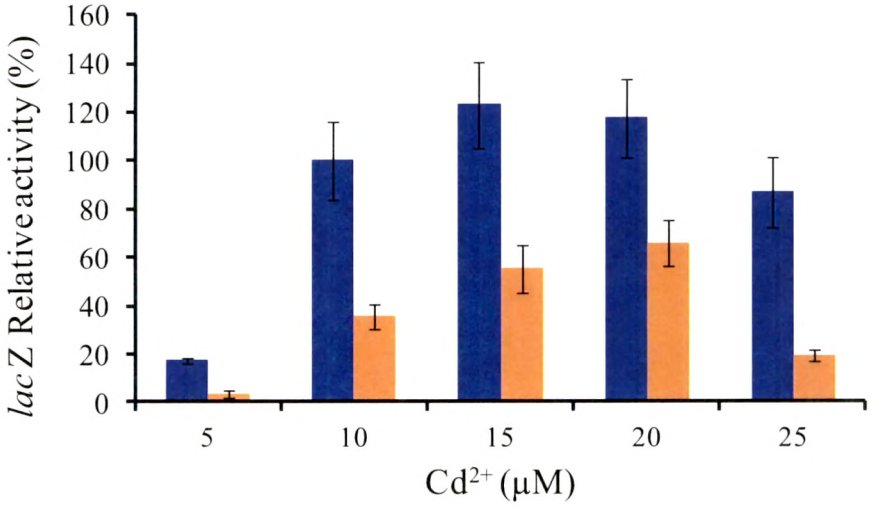

Fig. 3.25 Effect of Cd^{2+} on rec A promoter. Activity was assayed by using rec A- lac Z reporter in DR1. The relative activity is measured by normalizing the *lac* Z activity against the control. Blue bars : 1·5h & Orange bars : 3h of recovery.

Cd^{2+} is known to cause a single stranded break (Mitra and Bernstein, 1978) which was further affirmed by the proteomic analysis exhibiting the upregulation of *xth*A endonuclease in *E.coli* (Freianc et al., 1998). Trancriptomic analysis of *E.coli* exposed to Cd^{2+} exhibit upregulation of *recA*, *dnaN, dinJ*, and *uvrB* suggesting that the main repair pathway activated by Cd^{2+} is the nucleotide excision repair system, which typically responds to UV and is characterized by involvement of the *uvr* system (Wang et al., 2005). Similar gene expression has been observed in DR1 emphasing the role of recombinational and base excision repair for the cells exposed to Cd^{2+}(Joe et al., 2011).

3.3.7 Effect of Cd^{2+} on transcriptional regulator, PprI and Ppr M in DR1

Ppr I is a transcriptional regulator in DR1 that regulate the expression of *rec*A and is highly expressed in irradiated cells of DR1 (Earl et al., 2002; Ohba et al., 2005). Recently it was observed that PprI acts through PprM (Ohba et al., 2009) that

enhances the expression of Ppr A, which in turn activates catalase (Kota and Misra, 2006). However Ppr M has no effect on the activity of recA. The effect of Cd^{2+} toxicity on *ppr*I$^-$ and *ppr* M$^-$ mutant (Fig. 3.27), shows *ppr*I$^-$ mutant exhibited increased sensitivity to Cd^{2+} with a D_{50} of 0.49µg/ml (2.6 µM) which is less than *rec*A$^-$ mutant or *sod*A$^-$ mutant. As shown in Fig. 3.26, PprI regulates both catalase, through Ppr M, and Rec A further affirming the fact that Cd^{2+} affects both ROS combating enzymes as well as DNA repairing enzymes.

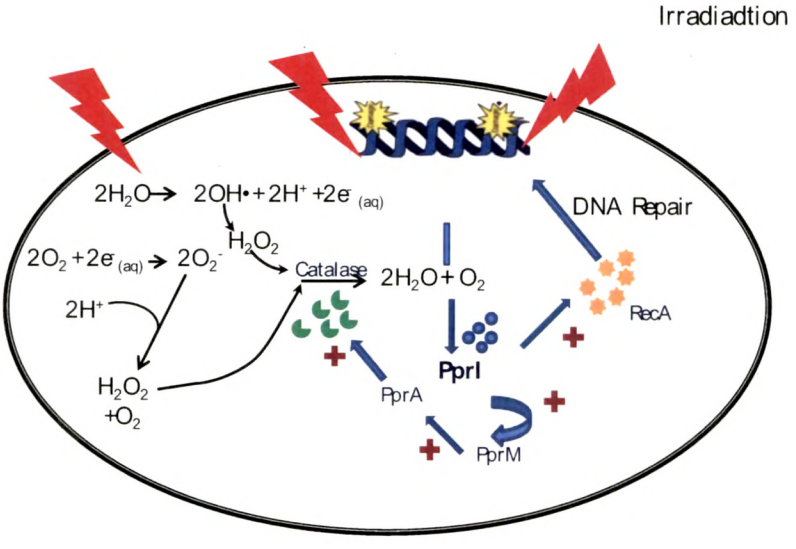

Fig. 3.26 PpR I mediated control of rec A and catalase activity in DR1, (+) indicates the positive regulation of the genes (compiled from Slade and Radman, 2011).

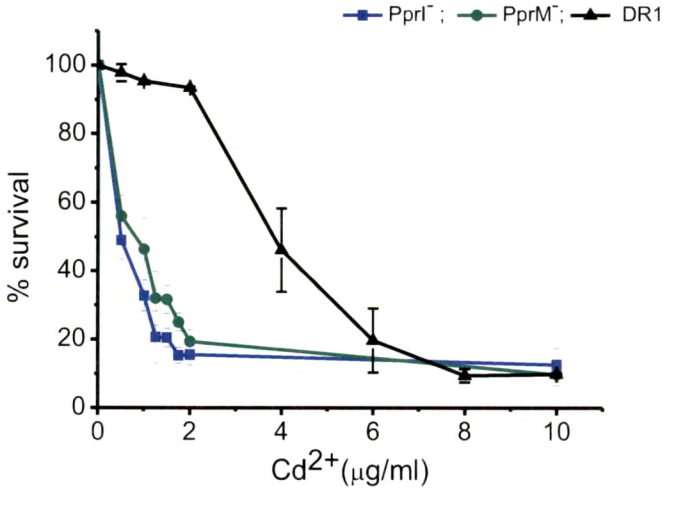

Fig. 3.27 Cd^{2+} toxicity in PprI$^-$ and PprM$^-$ mutant of DR1.

3.3.8 Protein profiling in response to Cd^{2+} in DR1

The apparent change in response to Cd^{2+} stress during stationary phase in DR1 was appalling as it is considered that most of the bacterial cultures tend to be resistant to external stress in stationary phase due to inherent upregulation of several stress regulons during stationary phase (Nystrom, 2004; Ishihama et al., 1997). Sukhi et al., (2009) reported the differential radiation resistance in DR1 influenced by the growth state, which was attributed to the lack of stationary phase specific sigma factor, σ^S. To gain further insight into the mechanism that may operate for Cd^{2+} sensitivity during the stationary phase protein profiles of the Cd^{2+}-stressed cultures grown under different growth phases was analysed. Cd^{2+} affected the proteome wherein a large majority of proteins were either repressed or had undergone degradation. In particular, absence of proteins in the range of 29 kDa and 14 kDa indicate degradation of the proteins while those in the range of 68-43 kDa appear to have repressed with respect to other conditions, stationary phase, log phase and Mn^{2+} amended to the log hase cultures, used in the study (Fig. 3.28). On the contrary several proteins appeared to be strongly upregulated in case of stationary phase cultures as opposed to log phase cultures. Mn^{2+} exposed culture appeared similar except for a single band > 18.4 kDa appears to be strongly upregulated (Fig. 3.28).

Analysis of 2-D gels using Melanie 7 software taking log phase treated cells as the reference gel showed that, of the 41 spots detected by the software in the log phase protein sample, 32 % were common with other conditions while Cd^{2+} treated cells have surprisingly only a single protein matching with reference log phase cells of DR1. Stationary phase cells and Mn^{2+} treated cells showed 23 % and 36 % respectively similarity to the log phase proteome (Fig. 3.29).

In accordance to the SDS-PAGE profile, Cd^{2+} treated cells show a decline in the number of proteins spots. Spot detected in Fig. 3.30 panel 1 was completely degraded under stress condition, while in Fig.3.30 panel 2 the spot in log phase was repressed in all stress conditions. Mn^{2+} and Cd^{2+} affected proteins showed appreciable similarity as reflected in Fig. 3.30 panel 3. Some common proteins were detected under Mn^{2+}, Cd^{2+} induction and stationary phase cultures as depicted in Fig. 3.30 panel 4.

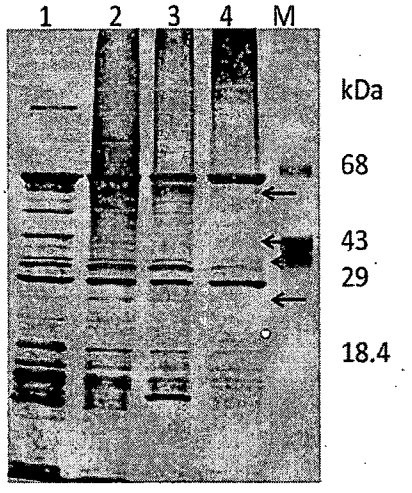

Fig. 3.28 SDS-PAGE analysis of total cellular proteins from DR1 treated with Cd^{2+} under different growth conditions, 1. Stationary phase; 2. Log phase; 3. Log + 100 μ M Mn^{2+}; 4. Log + 2.5 μ M Cd^{2+}

There was overall large amount of similarity amongst the proteins expressed during stationary phase, Mn^{2+} induced and Cd^{2+} induced cultures of DR1, therefore it can be concluded that exogenous Mn^{2+} can also exert stressful conditions in DR1. No spots were detected exclusively for both stationary phase cultures and Cd^{2+} affected cells indicating that DR1 has more generalised response to combat the Cd^{2+} stress and no unique mechanism to combat Cd^{2+}. Further identification of these proteins may incur insight into the exact mechanism to handle stress in DR1. Heat shock proteins, Mn^{2+} superoxide dismutase, Clp B protease form a common response proteins expressed under Cd^{2+} in *Campylobacter jejuni* (Kaakoush et al., 2008) and in *Corynebacterium glutamicum* (Fanous et al., 2008). These observations indicate that Cd^{2+} does induce oxidative stress and thereby damaging proteins which is affirmed by the induction of heat shock proteins as well as protease such as ClpB

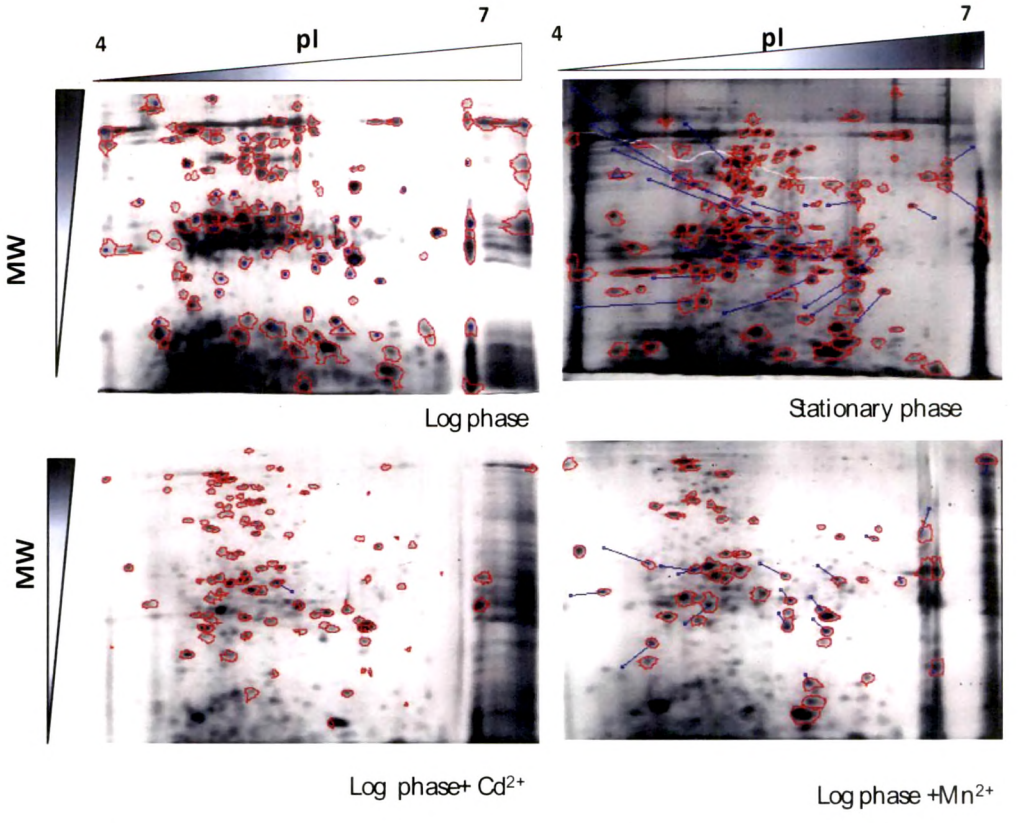

Fig. 3.29 2D gel electrophoresis of DR1 under different growth conditions. The analysis was done using Melanie 7. The spots marked in red were used for analysis while the blue vectors represent the common proteins detected with log phase as reference gel.

3.3.9 Cd^{2+} and Mn^{2+} binding proteome of DR1

The metallo-proteome is defined as the set of proteins that have metal-binding capacity by being metalloproteins or having metal-binding sites. A metalloproteome may include proteins that are unique for a metal as well as those that may be shared with some metal. The proteins that bind metal are more susceptible to metal catalysed oxidative damage. Affinities of proteins for metals have a tendency to follow a universal order of preference, which for essential divalent metals is the Irving–Williams series, given as: Mg^{2+} and Ca^{2+} (weakest binding) < Mn^{2+} < Fe^{2+} < Co^{2+} < Ni^{2+} < Cu^{2+} > Zn^{2+}. By restricting the effective concentration of the competitive metals at the top of the Irving–Williams series, metal-binding sites remain available to less-competitive, weak binding inorganic ions (Waldron and Robinson, 2009).

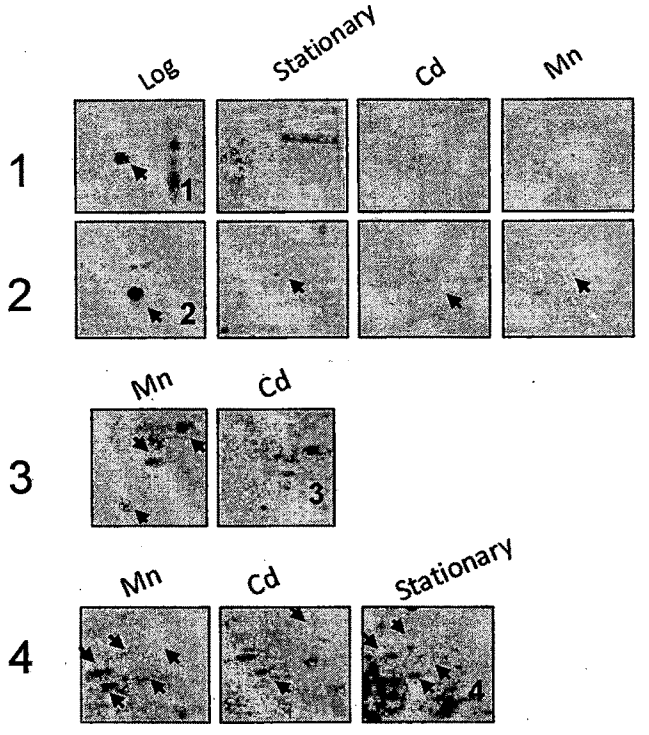

Fig. 3.30 Proteins differentially expressed under different growth conditions in DR1 panel 1). Protein spots (indicated by arrow) differiantially expressed in log phase but not present in other conditions tested; 2) Indicates protein that are strongly repressed in log phase but repressed under all other growth conditions; 3) Proteins expressed both in presence of Mn^{2+} as well as Cd^{2+}; 4) Proteins that are comonly expressed under stationary phase , Mn^{2+} and Cd^{2}

DR1 accumulates large amount of Mn^{2+} intracellularly (Daly et al., 2004; Ghosal et al., 2005), This is supported by the fact that several enzymes of DR1 employ Mn^{2+} as co-factor such as the class II fructose-1,6-bisphosphate aldolase uses Mn^{2+} instead of Zn^{2+} as cofactor (Zhang et al., 2006), Proteins differentially expressed under different growth conditions in DR1 employ Mn^{2+} as co-factor as in RNA ligase (Martins and Shuman, 2004), (di)adenosine polyphosphate hydrolase (Fisher et al., 2006), UV endonuclease β (Evans and Mosley, 1995), DNA pol.X (Blasius et al., 2006), Mn-SOD (Juan et al., 1991), NAD dependent DNA ligase (Blasius et al., 2006). Assuming that Cd^{2+} may compete with Mn^{2+} and other essential metals for binding with proteins, it was of interest to sudy the Cd^{2+} and Mn^{2+} binding proteonme of DR1. To study the metallo proteome IMAC was employed.

As seen in the Fig. 3.31 there is appreciable similarity between the proteins that are bound to Mn^{2+} and Cd^{2+} under all the conditions tested while no proteins were

retained on the control column, indicating the possibility of several Mn^{2+} interacting protein that can bind Cd^{2+} as well. Apart from the common proteome represented under conditions listed in Fig. 3.31 the proteins represented between 49 and 23 kDa formed a unique fingerprint of the stationary phase culture not represented in any other proteome. Of the stationary phase proteome a band > 97 kDa was found only in the elutate of Cd^{2+} binding proteome while a band of 29 kDa was found to be unique to log phase Mn^{2+} binding proteome not represented in the respective Cd^{2+} proteome. Mn^{2+} induced proteome also reflected unique proteins binding to Cd^{2+} only and not Mn^{2+} in the range of 66 kDa and 43 kDa, suprinsigly there was no observable difference reflected in Mn^{2+} and Cd^{2+} binding proteins in Cd^{2+} induced proteins. Sequence and consequent structural analysis shall be able to consolidate our results.

In-silico analysis of the band pattern from the individual proteome was performed which revealed the similarity between Cd^{2+} induced, Mn^{2+} binding proteins as well as Cd^{2+} binding proteins to the stationary phase Mn^{2+} binding proteome. This justifiies the fact that there could be several targets for Cd^{2+} during the stationary phase which possibly explain the sensitivity of the stationary phase cultures to Cd^{2+} than the log phase. Fig. 3.32

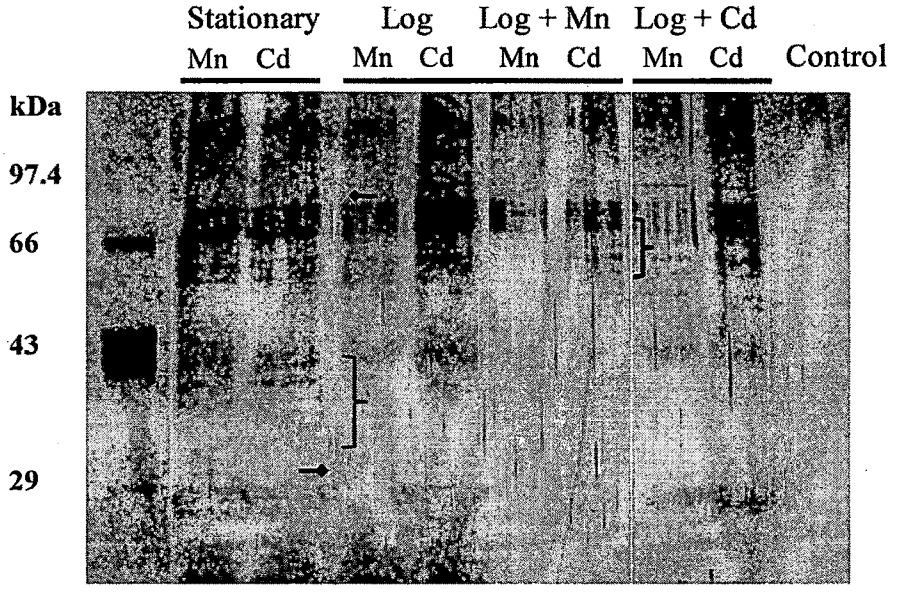

Fig. 3.31 SDS PAGE of Mn^{2+} and Cd^{2+} binding proteins in DR1 obtained by IMAC.

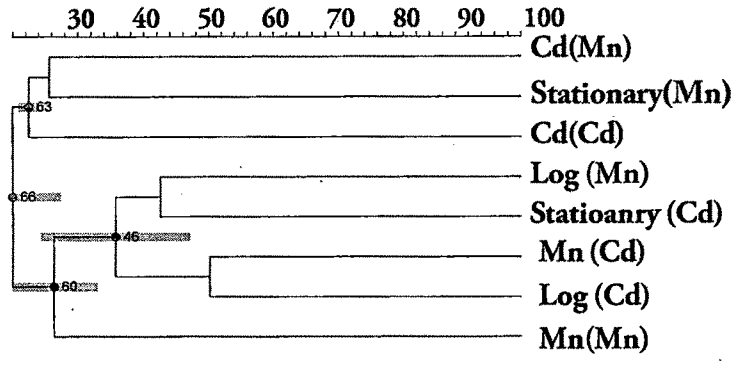

Fig. 3.32 Dendrogram obtained from In silico analysis of the proteins represented in Fig. 3.31. UPGMA was employed to generate the dendrogram, the values at the nodes indicate the % similarity.

A comparison between the metallo-proteome of specific metal under different growth conditions reveal that proteins binding to Mn^{2+} column under all growth condition (Fig. 3.33 (A)) revealed the presence of bands indicated as band 1 (97.4 kDa), band 2 (>97.4 kDa), band 3 (43 k Da) and a doublet band 4 (>43 kDa) unique to stationary phase cultures while band 5 was only represented in the Cd^{2+} induced cultures. Presence of common Mn^{2+} biding proteome reflect a large number of proteins are capable of binding to Mn^{2+} and might be essential for the normal growth. However there were only two unique bands binding to the Cd^{2+} column each elonging to Mn^{2+} and Cd^{2+} induced cultures of DR1 (Fig. 3.33(B)).

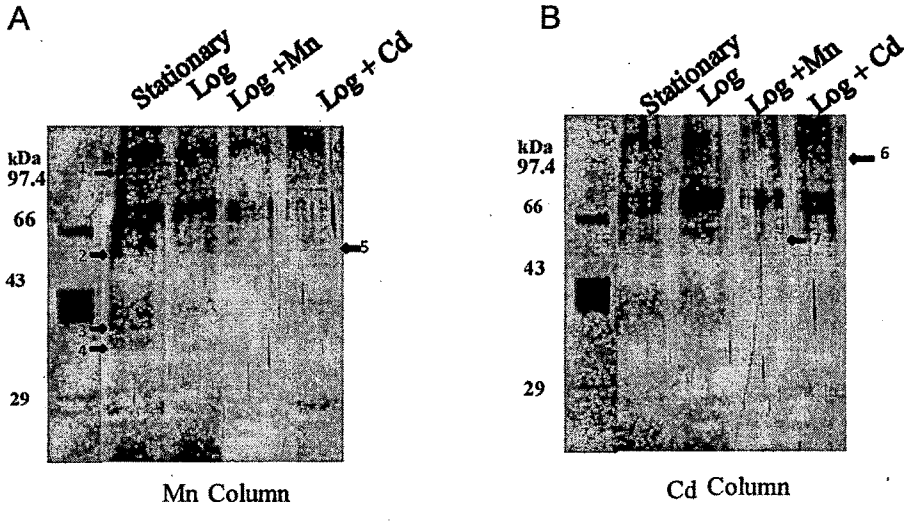

Fig. 3.33 IMAC purification of A) Mn^{2+} binding proteome of the DR1 cells; B) Cd^{2+} binding proteome of DR1 cells. Arrows indicate unique bands discussed in the text.

3.4 Conclusion

DR1 is considered as the most potential candidate for the bioremediation of nuclear waste sites. DR1 and other radiation resistant organisms employed in the study were found to be sensitive to Hg^{2+} and Cd^{2+}. Amongst the radiation resistant organisms examined for Hg^{2+} toxicity Grk2 was found to be most resistant, while Grk4 was most resistant to Cd^{2+}. DR1 exhibited comparatively higher level of resistance for Cr^{6+}.

Cd^{2+} toxicity in DR1 was affected by growth phase with stationary phase cells being more sensitive than the exponential phase. Stationary phase of DR1 cells have been earlier shown to be more radiation sensitive as opposed to the exponential phase cultures (Sukhi et al., 2009). The toxicity of stationary phase cells was ameliorated by addition of exogenous Mn^{2+}, indicating the possible competitive role of Mn^{2+}

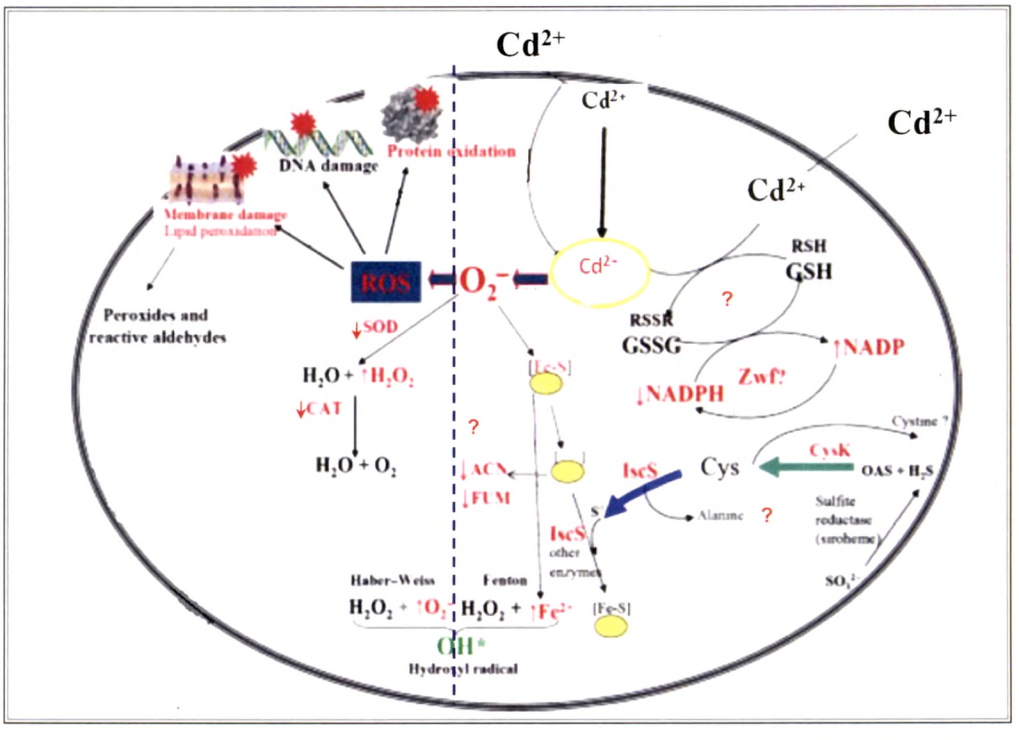

Fig. 3.34 Effect of Cd^{2+} on different ROS pathways in DR1. The pathways marked with question mark, right of the demarcated line, may play a possible role in tolerance towards Cd^{2+} but need to be adderessed.

Cd^{2+} is known to elicit oxidative stress most likely indirectly by replacing Fe, from Fe-S clusters, free Fe is capable of generating and propagating ROS by promoting Fenton's chemistry. In our studies Cd^{2+} was demonstrated to elicit ROS response leading

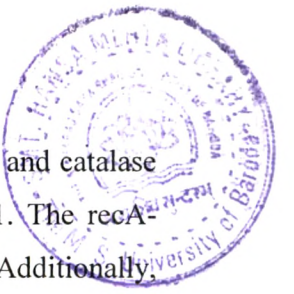

to oxidative damage to proteins and lipid peroxidation. Diminution in SOD and catalase activity with concomitant increase in ROS explains Cd^{2+} toxicity in DR1. The recA- mutant was found to be sensitive to Cd^{2+} as compared to the wild type. Additionally, dose-dependent response of recA-*lac* Z reporter assay in DR1 indicates that Cd^{2+} is capable of asserting DNA damage in DR1. A concerted effect of increase in ROS, inactivation of the ROS combative enzymes and DNA damage further aggravates the Cd^{2+} stress in DR1. Due to high Requirement of high intracellular Mn^{2+} by DR1 implies existence of several proteins that may interact with Mn^{2+} which may act as potential targets for Cd^{2+} toxicity. This was affirmed by the presence of several common proteins that bind both Mn^{2+} and Cd^{2+} under varying growth conditions. Further studies needs to be undertaken to reveal the identity of the Cd^{2+} binding proteins to understand the exact mechanism of Cd^{2+} toxicity in DR1. Fig. 3.34 summarises the observations in this study.